Hydrothermal liquefaction of lignocellulosic biomass to produce biofuels

by

Ankit Mathanker

A thesis submitted in partial fulfillment of the requirements for the degree of

Master of Science

in

CHEMICAL ENGINEERING

Department of Chemical and Materials Engineering
University of Alberta

ABSTRACT

There is an increasing need of clean renewable energy sources to address the growing problems of greenhouse gas emission, global warming and climate change. The rapid consumption of fossil fuel resources has also contributed to toxic emissions and raised a question on sustainability of present fuels. Hence, alternative renewable fuels such as biofuels have been considered as a promising low pollution source. Biomass is composed of the green carbon i.e. carbon that belongs to the present biological cycle, making it a cleaner fuel. Biomass has an inherent energy that comes from the sun and has possibility to regrow in a short period of time. Lignocellulosic biomass mainly derived from agricultural and forest can be processed through pyrolysis, gasification, steam reforming and hydrothermal liquefaction to obtain high energy density biofuels.

Predominantly, all biomass materials contain high moisture, which makes the hydrothermal liquefaction as the most effective technique for conversion of biomass to biofuels such as bio-oil, hydrochar and gases. In this work, hydrothermal liquefaction process was used for conversion of lignocellulosic biomass (corn stover) into liquid, solid and gaseous fuels at moderate temperature in the range of 250 – 375 °C, final pressure (P_f) in range of 1100 – 3400 psi and retention time (t_r) in range 0 – 60 min. The key focus of this research work is to understand feedstock properties, develop experimental methodology for hydrothermal liquefaction and apply it for conversion of biomass to biofuels. The study also attempts to optimize the process parameters with an aim to obtain quantitatively and qualitatively better biofuels.

The experiments were performed in a 250 mL, high pressure autoclave batch reactor having temperature and pressure upper limit of 500 °C and 5000 psi (34.47 MPa) respectively. An inert nitrogen environment was maintained. The final recovered slurry was processed through a detailed

separation procedure in order to obtain the bio-oil and hydrochar separately for analysis. In order to understand the properties of products, characterization tests such as elemental analysis and GC-MS was performed on bio-oil and elemental analysis, FTIR and SEM were carried out on hydrochar.

The quantitative results obtained at different operation conditions gave a highest yield of heavy oil (29.25 wt.%) obtained at 300 °C, final pressure, P_f, of 2200 psi and 0 min retention time. The highest yield of hydrochar (30.21 wt.%) was obtained at 350 °C, P_f of 3150 psi and soak period, t_r, of 15 min. Based on elemental analysis and energy calculation, highest carbon content and higher heating value for heavy oil was 76.32 wt.% and 35.13 MJ/kg at 375 °C, P_f of 600 psi and t_r of 15 min; and for hydrochar it was 68.23 wt.% and 24.7 MJ/kg at 350 °C, P_f of 3150 psi and t_r of 15 min. The GC-MS results for heavy oil indicated that majority of the compounds were phenolic in nature. FTIR results confirmed the decomposition of protein and carbohydrate and formation of new aromatic bonds in hydrochar during HTL. The morphology results for different hydrochar indicates the breaking of fibrous structure and formation of a more porous material. Even though, quality of oil obtained in this study was good, more studies need to be carried out in a direction to upgrade oil by reducing the oxygen content and increasing the higher heating value; moreover, developing better understanding by analyzing viscosity and total acid number value.

PREFACE

This thesis is an original research conducted by the author, Ankit Mathanker at the University of Alberta, Edmonton, Canada. Most of the experiments and characterizations were conducted at the Department of Chemical Engineering, with elemental analysis conducted at the Department of Chemistry, morphology test conducted at the Department of Earth and Atmospheric Sciences and the FTIR analysis conducted at the Oil Sands and Coal Interfacial Engineering Facility, University of Alberta.

Dr. Rajender Gupta was the principal advisor on this work and was involved at every step during the research in development of process, implementation and documentation edits.

ACKNOWLEDGEMENTS

I would like to thank my supervisor, Dr. Rajender Gupta for taking me in the team and providing me with an opportunity to conduct research on this project for the Master of Science thesis. A sincere gratitude for your academic and personal guidance. Your knowledge, guidance, intellectual questioning, active participation and positive (go for it) attitude helped me to complete this thesis timely. I will carry on the teaching lesson that I gained from you about effective mentor-mentee conduct throughout my career. I also thank Dr. Amit Kumar for his support and suggestion in this work.

I would like to thank the Future Energy System, University of Alberta for providing financial support to carry out this research work. Furthermore, I would like to acknowledge the support of Faculty of Graduate Studies and Research, and, Graduate Student Association, University of Alberta for providing financial support to my conference travel and accommodation.

I am highly thankful to Dr. Deepak Pudasainee for his teaching and valuable suggestion throughout this work. I thank Dr. Pudasainee to always be there to review my work and for teaching me to handle Autoclave reactor, BET and LECO TGA. I am grateful to Dr. Madhumita Patel, Dr. Vinoj Kurian and Dr. Md Khan for various discussions and suggestions related to experimental process and lab conduct. A special thanks to Ni Yang and Garima Chourasia for teaching me to operate FTIR analysis and GC-TCD respectively. I want to acknowledge assistance of Nathan Gerein and Guibin Ma who helped me with SEM analysis. I am also thankful to Vinay Khatri, Lisa Nikolai and Samuel Yue for there much needed discussion on operation of GC-MS. A warm thanks to Manjot Gill and Ananthan Santhanakrishnan for being the best office and lab partners and their involvement in much needed brainstorming to figure out various solutions.

I want to acknowledge and thank my friends at the University of Alberta for sharing the burden and joy of graduate school with me. Thank you so much folks- Anuja, Karthik, Harish, Aakash, Sahil, Soumya, Duo, Shirley, Shruthi, Filipe, Himanshi, Yuvraj, Anagha, Snehlata, Yang Wu, Manika, Omnath, Shruti, Akanksha, Oliver, Adriana and all my Toastmasters, Unitea and Pokémon go members. Thanks for your support and encouragement.

I am very thankful to Dr. Arunkumar Samanta and Dr. Gopal Pugazhenthi who supported my application with their recommendation for University of Alberta. I also thank them for providing undergraduate research opportunities which prepared me for this journey at University of Alberta.

Last but not the least, I would like to express my gratitude and thank my parents, uncle-aunt and my brother for supporting me in this journey. It was a tough road coming to a new country for studies and I would have crashed miles before if you haven't been there to back me.

TABLE OF CONTENTS

LIST OF FIGURES

LIST OF TABLES

LIST OF ACRONYMS

HTL – Hydrothermal liquefaction

t_r – Retention time

P_f – Final pressure

P_i – Initial pressure

HC – Hydrochar

HO – Heavy oil

AO – Aqueous oil

HHV – Higher heating value

HC(300,300,15) – Hydrochar obtained at reaction temperature 300 °C, initial pressure 300 psi and retention time 15 min

HO(300,300,15) – Heavy oil obtained at reaction temperature 300 °C, initial pressure 300 psi and retention time 15 min

HC(300,300,15) – Aqueous oil obtained at reaction temperature 300 °C, initial pressure 300 psi and retention time 15 min

Chapter 1 : Introduction

1.1 Motivation and background

The two main challenges of the twentieth century are the increasing greenhouse gas emission and decreasing predominant source of commercial fossil fuels. The unprecedented rate of global CO_2 emission, as a greenhouse gas, has been leading to gradual increase in temperature and affect climate unpredictability [1]. Fossil fuels are the major sources of energy at present and they are the most dominant contributor of greenhouse gases and toxic pollutants emission into the atmosphere [2, 3]. Increasing dependency on fossil fuels possesses a danger to the human health, environment and sustainability. Even with minimum growth rate of 1 % per annum the proven resource of fossil fuels is predicted to vanish by the year 2100 [4]. The world population is predicted to increase from 7.7 billion in 2019 to 9.7 billion in 2050 and eventually become 10.9 billion by 2100 [5]. The total consumption and per capita consumption of energy is projected to increasing with increase in population [6]. Hence, in order to mitigate greenhouse gas emission and to cope with the increasing energy requirements, there is an increasing demand for renewable fuels.

Renewable fuels or sustainable energy source derived from biomass, biomass waste is attracting a lot of attention as biomass is CO_2 neutral and has energy rich chemical composition [7]. In last two decades, many major studies have been conducted to utilize biomass as fuel, upgrade biomass to increase energy value, produce value-added chemicals/fuels and understanding reaction mechanism of biomass conversion [8, 9, 10]. The first-generation biofuels such as ethanol and biodiesel comes from mostly edible biomass such as sugarcane, oilseeds, corn, whey, barley, potato wastes and sugar beets etc. [11]. The second-generation biofuels are fuels produced from

agricultural (non-edible) residue, forest residue and non-forage crops. Lastly, the third-generation biofuels are the fuels that are developed from algal biomass. The first-generation feedstocks are majorly edible products; hence its utilization gives raise to many issues such as decrease in the availability and price increment for edible products. Production of third-generation biofuels requires separate feedstock growth environment increasing the total cost of production. Hence, production of biofuels from second-generation agricultural and forest feedstock is the most promising route.

The agricultural and forest biomass residues are renewable and sustainable in nature. It is expected to play a major part to meet present and future energy demand. The agricultural sector ends up producing considerably large amount of biomass waste annually. Some part of agricultural residue is used in animal husbandry and majority of it is left aside posing major concern not only for waste management but also from emission point of view. The use of these lignocellulosic residue using conversion technologies to increase their energy density can help to meet energy needs and solve waste management issue.

The present ways to utilize agricultural and forest residue is to use it for co-combustion or to use conversion technologies such as pyrolysis and gasification. The high amount of inherent moisture content in lignocellulosic feedstock obtained from agricultural and forest sector requires drying to reduce moisture before conversion which increases the overall cost of the process. In order to avoid additional steps of moisture removal there is a need to research a more viable conversion path. Many researchers have studied hydrothermal liquefaction (HTL) process to upgrade properties of feed and to produce value-added products. The HTL is a high temperature and high pressure process which occur in presence of water. The region of Saskatchewan (17.38) and Alberta (11.58) produces an estimated total of 28.96 million dry tonne yr^{-1} of agricultural

residue, which can be potentially used for biofuels production [31]. Thus, this research work aims at studying the potential of HTL process to handle high moisture lignocellulose feedstock obtained in Alberta region to produce biofuels.

1.2 Research objectives

The objective of this study focuses on:

- Understanding the properties of the corn stover by conducting initial characterization test to obtain composition analysis
- Understanding the effect of various HTL process parameters such as temperature, pressure and retention time on product yield and quality
- Understand the product quality by conducting various characterization tests such as elemental analysis, GC-MS, FTIR and morphology studies.

1.3 Thesis outline

The thesis is divided into 5 chapters:

Chapter 1: Introduces the background and need for this study and brief about the present status of research in this area, i.e. hydrothermal liquefaction of biomass for biofuel production.

Chapter 2: This chapter provides a brief literature review about different biomass feedstocks, availability of feedstock in Canada, structural and elemental composition of various biomass, different available processes for the conversion of biomass to biofuels and finally the effect of various process parameters on hydrothermal liquefaction.

Chapter 3: The experimental section discusses about feed preparation, experimental procedure, characterization techniques for analysis of feed and products.

Chapter 4: In this chapter the results obtained at different conditions are presented, discussion on effect of process parameters and characterization results is presented and supported based on available literature.

Finally, conclusion provides the outcomes obtained in this this study and possible area of research is discussed in future scope.

Chapter 2 : Literature Review

2.1 Biomass feedstock

Biomass is a vast renewable resource comprised of all the organic hydrocarbon material derived directly or indirectly from the process of photosynthesis. Biomass is a generic term for the plant (flora) and animal (fauna) biomass present on the earth. Biomass is mainly composed of carbon, hydrogen and oxygen with a comparatively insignificant amount of nitrogen, sulfur and phosphorus [12]. It also contains inorganic impurities in the form of ash. Biomass can mainly be classified based on (i) its presence in nature (vegetation type) as shown in Figure 1 and (ii) utility of biomass residue.

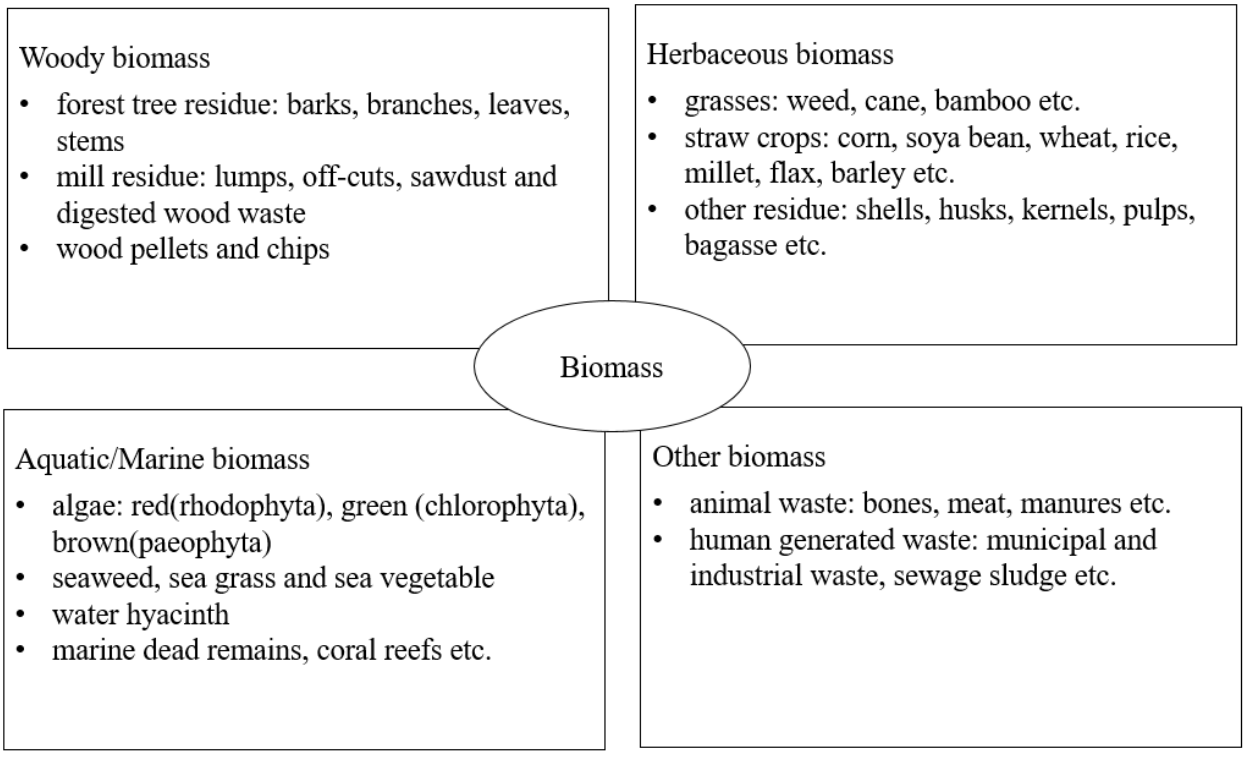

Figure 1 Biomass classification based on existence in nature [13]

Based on utility of biomass, it is mainly divided into two main categories:

i) First-generation biomass: edible parts of oil seeds crops, vegetable crops and sugar crops

ii) Second-generation biomass: lignocellulose biomass (agricultural, forest, energy crop) and other non-food parts of crops

At present, biomass is seen as a significant source of energy to contribute in an energy outlook. The first-generation biomass is mainly utilized for dietary needs of human beings and is available in a limited amount to meet the government food budget. The limited supply of food feedstock restricts its tailoring to produce energy and chemicals. Second generation biomass is available in abundant and can be used to produce renewable energy to replace a part of conventional fossil fuels. Table 1 discusses about various types of second-generation biomass that can be used to produce fuels, energy and other chemicals [14].

Table 1 Classification of second-generation biomass for energy and fuel purposes

Supply sector	**Type of biomass**	**Raw feedstock**	**Useable final product**
Agriculture	Lignocellulosic woody dedicated energy crop	Willow, poplar, black locust	Fuel in powerplant [15]; Chemicals [16]
	Lignocellulosic herbaceous dedicated energy crop	Shrubs and grasses; giant reed	Bio-oil [17], Hydrochar [17]
	Dedicated oil energy crop	Sugar and cane beet; sweet sorghum	Biocrude oil [6,9]
	Dedicated starch energy crop	Corncob, potatoes; sunflower	Biocrude [19]
	Agricultural residues	Sugarcane bagasse; straw (wheat, corn,	Liquefaction oil [7,9];

		millet); pulps; palm trunks and fronds	methane production [8]; solid biofuel [22]
	Livestock waste	Manure, bones, meat, fat	Biocrude oil [10,11] Glycerin [24]
Forestry	Forest residue	Pine wood; aspen wood	Biocrude oil [12,13]
Industry	Wood residue, industrial by-products	Waste from timber mills (bark, stripes, sawdust etc.)	Biooil, biochar [26–29]
	Food residue	Fats, Proteins, Processed vegetable wastes	Biodiesel, ethanol, methane [30]
Other	Marine biomass	Algae	Biocrude oil [23] Gas [23]

2.2 Biomass in Canada

Canada is rich in biomass resources. As per study conducted by Li et al. [31] for the period 2001 – 2010, Canada produced a total of 168.27 million dry tonne (MDT) yr^{-1} of field and non-forage crops. Out of which, a total of 48 MDT yr^{-1} was available as agricultural residue for biofuel production. The region of Saskatchewan (17.38) and Alberta (11.58) produces an estimated total of 28.96 MDT yr^{-1} of agricultural residue, which can be potentially use as biofuels [31].

2.3 Structural composition of biomass

As discussed in section 2.1, biomass is a generic term for all the organic hydrocarbon materials linked with photosynthesis. Based on the natural origin of biomass, as discussed in Figure 1, the structural composition and the elemental composition of biomass greatly varies.

Biomass originating from plant and plant-based material obtained from agricultural, forestry and pulp and paper industry sector is mainly called lignocellulosic biomass. Majorly lignocellulosic biomass is composed of cellulose, hemicellulose, lignin and some extractives. A small fraction of inorganic mixture is also present in biomass [32]. Conversion of biomass to solid, liquid and gaseous fuels predominantly depends on the fraction of cellulose, hemicellulose and lignin present in it. These three are the main cell wall components responsible for the physical properties (mechanical support and strength) for plants. Table 2 presents composition of cellulose, hemicellulose and lignin in different biomass.

The composition of biomass significantly affects the yield of biofuels. The fraction of cellulose and hemicellulose contribute majorly to the bio-oil yield, as they both tend to degrade at intermediate temperature; whereas lignin majorly contributes to solid char, due to its high degree of polymerization that needs elevated temperature for depolymerization [33].

Table 2 Structural composition of different biomass feedstock

Biomass	Cellulose	Hemicellulose	Lignin	Reference
Forest Biomass				
Softwood	44.5	21.9	27.7	[34]
Switchgrass	35.4	26.5	18.2	[34]
Shrub (Salix psammophila)	55.45	18.89	25.49	[17]
Aspen wood	47.14±0.86	19.64±0.11	22.11±0.17	[25]
Pine sawdust	40.2	21.9	28.4	[27]
Pine	36.7	26.1	27.5	[35]
Ash wood	39	21.9	26.3	[35]
Miscanthus	45.7	22.8	20.2	[35]

Birch	56.47	24.79	12.17	[36]
Oak	53.95	28.97	9.43	[36]
Eucalyptus	48	14	29	[37]
Spruce wood	50.8	21.2	27.5	[38]
Beech wood	45.8	31.8	21.9	[38]
Agricultural Biomass				
Sweet sorghum	36.17	19.68	17.66	[18]
Corn stover	38.1	25.3	20.2	[34]
Wheat straw	32.6	22.6	16.8	[34]
Sugar beet pulp	30±2.4	26.8±1.82	4.1±1.6	[34]
Palm frond	31	17.1	22.9	[22]
Palm trunk	39.9	21.2	22.6	[22]
Rice straw	41.33	24.6	9.22	[39]
Barley straw	46	23	15	[40]
Corn stalk	42.7	23.2	17.5	[41]
Peanut vine	44.99	18.23	11.76	[41]
Sweet sorghum	35	17	17	[38]
Hazelnut shell	25.9	29.9	42.5	[38]
Other Biomass				
Swine manure	3.8±1.4	27.3±2.2	3.6±1.3	[23]
Algal Mixture	14.4	3.5	5.7	[23]

2.3.1 Cellulose

Cellulose is the most common organic biopolymer and the main part of cell walls of the plant's cells, which is also known as glucan and glucosan [32]. Cellulose is a homo-polysaccharide represented by the general formula $(C_6H_{10}O_5)_n$ ($n \approx 10{,}000$), is formed by the linearly coupled D-glucopyranoside units connected by β-glyosidic linkages in a 1:4 fashion [7]. The molecular mass of cellulose unit is typically of the order of 10^6 $kg.kmol^{-1}$ [7]. The main forces holding several cellulose chains to form crystalline lattice are intrachain and interchain hydrogen bonds. A group of these chain bonded together forms cellulose microfibril [42]. Inside biomass, cellulose is stable and organized into microfibrils surrounded by hemicellulose and encased with lignin[43]. Increase in the density of packing leads to formation of crystalline regions, the crystalline region is non-accessible and is completely insoluble in aqueous solutions [44] and requires set of treatment known as mercerization [45] to make it hydrophilic. The non-crystalline region is mostly accessible and is first to be attacked during hydrolysis [13]. The partial cellulose unit along with inter and intra-hydrogen bond is shown in Figure 2.

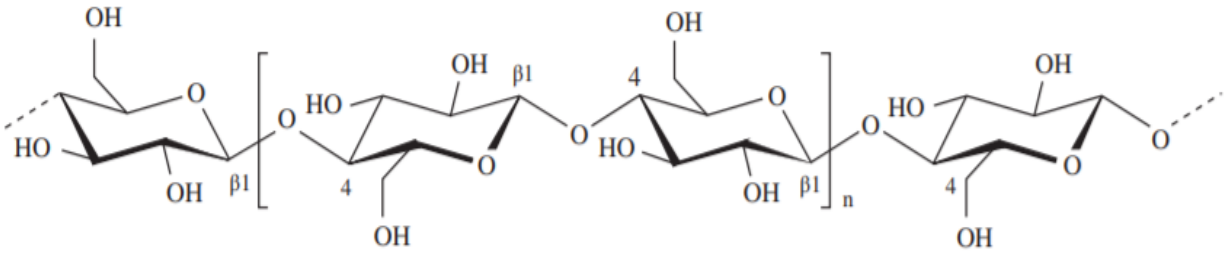

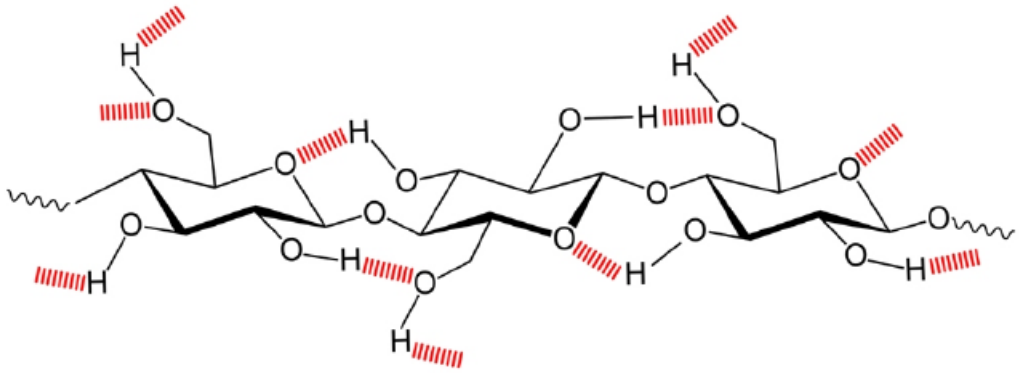

Figure 2 Cellulose structural unit (top) [7] , intra and intermolecular hydrogen bonding (bottom) [13]

Minowa et al. [46], performed hydrothermal liquefaction of cellulose and obtained that it decomposes quickly between 240 – 270 °C and no cellulose remained at over 280 °C. In general, the mechanism of cellulose decomposition starts with decomposition of cellulose to oligosaccharides and monosaccharides, and then oligosaccharides and monosaccharides to furans and other products, depending on the presence and absence of aqueous medium [18,21].

2.3.2 Hemicellulose

Hemicellulose are hetero-polysaccharides and the second most abundant component in plant biomass, which is mainly consist of D-xylose, D-glucose, D-mannose and D-galactose and other glycosyls as branched chain linked to this base chain. They are strongly linked to the surface of cellulose microfibrils and found in the cell wall regions of plants contributing to structural integrity [16,23]. Figure 3 shows an example structure for hemicellulose and the basic monomer units present in hemicellulose.

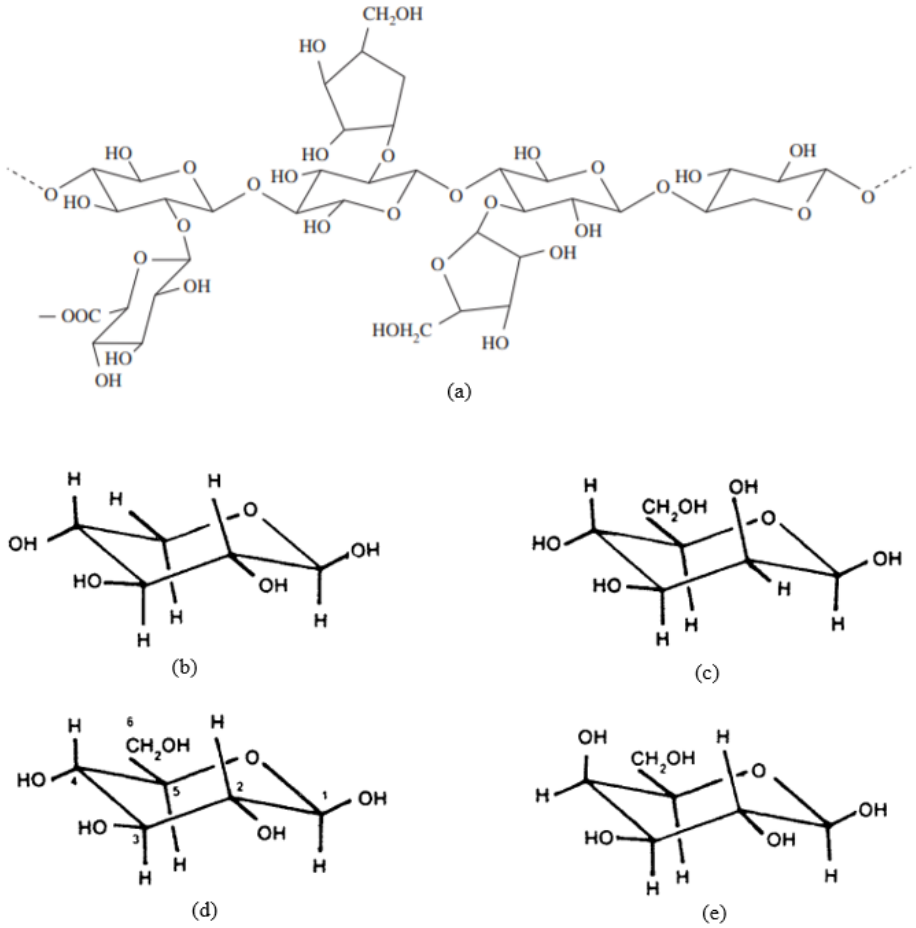

Figure 3 (a) Example structure for Hemicellulose [7]; monomer units of hemicellulose (b) D-Xylose, (c) D-Mannose, (c) D-Glucose, (d) D-Galactose [44]

The degree of polymerization in hemicellulose is in the range of 100 – 200 which is significantly lower in comparison to cellulose with an average of 9000 – 10000 [44]. Due to poor structural regularity and branched chains, the crystallinity of hemicellulose is weaker than that of cellulose [43]. The percentage of hemicellulose is lower in woody and herbaceous biomass than cellulose, whereas in manure the hemicellulose fraction is dominant [23] as shown in Table 2. Carpernter et al. [23], summarized, hemicellulose thermally decomposes between 180 to 350 °C producing, cellulose, char, gases and variety of furans, ketones and acids.

2.3.3 Lignin

Lignin are amorphous, highly intricated complex, composed of mainly aromatic polymers of phenylpropane units nonlinearly and randomly linked [49]. Lignin are three dimensional structure as shown in Figure 4, made of ether bonds and carbon-carbon linkages; their three main monomeric units are p-coumaryl alcohol, coniferyl alcohol and sinapyl alcohol [50]. It provides structural integrity, toughness to the cell walls of plants along with cellulose microfibrils and fills empty space between cellulose and hemicellulose playing a role of binder [51]. The p-courmaryl alcohol is minor component of both softwood and hardwood lignin and is commonly found in grasses, coniferyl alcohol is predominant component in softwood lignin; and coniferyl alcohol and sinapyl alcohol are both important part of softwood and hardwood lignin [48].

In general, lignin is relatively stable in thermal conversion and it has a larger higher heating value. The most common technique for lignin degradation and subunit composition analysis are acidolysis and thioacidolysis, and one of the non-degradative analytical techniques is thermogravimetric analysis [52]. One of the approach to convert lignin into low-molecular weight chemicals is hydrothermal liquefaction, based on reaction condition and reactor design lignin can be converted into high value products, such as phenolic derivatives and further into gases such as carbon monoxide, carbon dioxide, methane, ethane and other lower molecular weight side products[43].

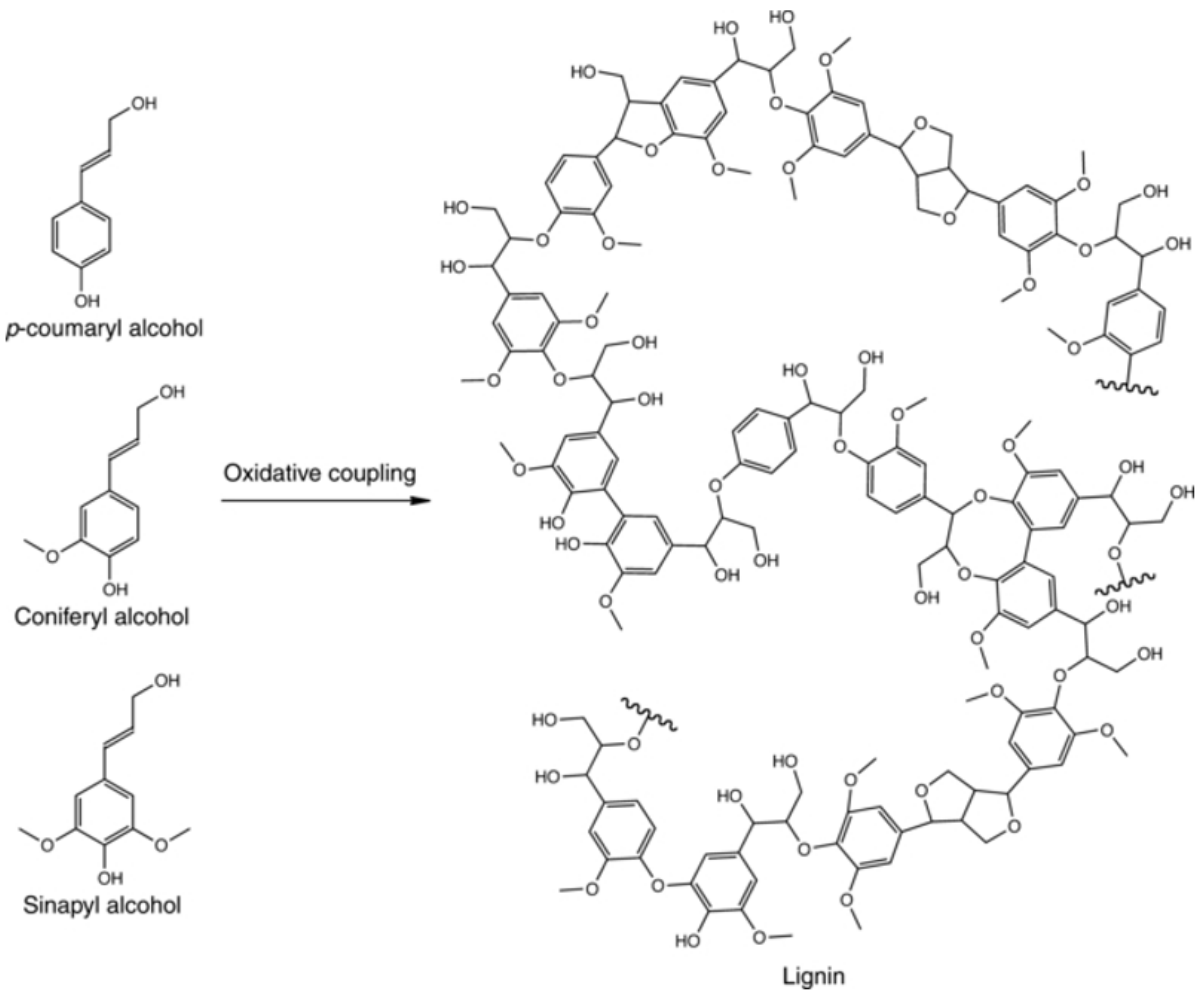

Figure 4 Monomeric units of lignin and lignin structural unit [50]

2.3.4 Extractives

Apart from the main compounds, biomass also contain extractives and minor organic compounds. The fraction of extractives depends on the type of biomass and varies greatly between plant feedstock, animal feedstock and solid waste. In general, extractives are chemicals present in cell wall consisting of fats, fatty acids and alcohol, phenols, aromatic amines, alkaloids, antioxidants, resins, waxes and other minor organic compounds such as lipids, proteins, nucleic acid and acetyls, vitamins, hormones, chlorophyll [2, 16,19].

2.3.5 Inorganic matter

The inorganic matter mainly contributes to the ash formation during conversion of biomass. The percentage and type of inorganic compounds present in biomass significantly varies between plant biomass and municipal solid waste. Even in plants mineral content shows high variability depending on genetic, environmental, physiological and morphological differences [32]. The inorganic matter is present in the form of chlorides, sulphates, oxalates, nitrates, carbonates [13]. The inorganic material is a mixture of wide range of elements; K>Ca>Mg be the primary one in that order and the other elements present includes P, S, N, Al, Fe, Cu, Zn, Pb, Rb, Sr, Ti, Ga, Ba, Co, Cr, Ni, Li, V, Zr and Sn [44].

2.4 Elemental composition of biomass

The organic compounds presented in section 2.3 are composed of Carbon, hydrogen and oxygen atoms and the small fraction of inorganic components. The decreasing order of abundance of these elements are commonly C, O, H, N and S. Table 3 presents a list of various biomass feedstock commonly used for HTL and their elemental composition.

Table 3 Elemental composition and ash content of different biomass

Biomass	C	H	N	O(diff)	S	Ash	Ref.
Forest Biomass							
Poplar	51.81	6.39	0.16	41.64	0.04	3	[15]
Willow	48.84	6.18	0.46	44.52	0.03	1.88	[15]
Black locust	51.51	6.44	0.63	41.42	0.05	3.33	[15]
Softwood	50.3	5.98	0.03	42.1	0.01	0.32	[34]
Switchgrass	46.9	5.54	0.62	42	0.7	4.28	[34]

Pine wood	46.6	6.3	0.1	47	-	<0.1	[53]
Shrub (Salix psammophila)	48.3	5.6	0.73	43.8	-	1.6	[17]
	50.39±0.8	6.19±0.0	0.19±0.0	43.23±0.0		0.46±0.	
Aspen wood	6	8	2	8	-	02	[25]
					<0.0		
Pine sawdust	52.5	6.32	0.1	40.6	5	0.4	[27]
Pine	51.5±0.3	5.8±0.2	0.2±0.06	42.3±0.1	-	0.3±0.1	[35]
Ash wood	49.6±0.7	5.4±0.5	0.3±0.05	43.2±0.6	-	1.5±0.1	[35]
Miscanthus	48.3±0.7	5.6±0.6	0.3±0.04	43.0±0.6	-	2.9±0.1	[35]
Birch	44.41	3.48	0.27	36.65		0.76	[36]
Oak	45.37	5.03	0.28	41.29	0.01	0.24	[36]
Spruce wood	51.9	6.1	0.3	40.9	-	1.5	[38]
Beech wood	49.5	6.2	0.4	41.2	-	1.4	[38]
Agricultural Biomass							
Sugarcane bagasse	45.9	6.9	0.26	46.6	0.34	6.1	[20]
Corn stover	46.7	5.49	0.67	38.4	0.1	8.59	[34]
Wheat straw	43.9	5.26	0.63	38.7	0.16	10.2	[34]
Sweet sorghum	41.3	5.39	1.32	51.98	-	4.59	[18]
Sugar beet pulp	38.6	5.9	1	54.5	-	14.4	[53]
Palm frond	47.2	5.9	0.2	46.6	0.1	1.8	[22]
Palm trunk	47.5	5.9	0.5	45.9	0.1	2.2	[22]
Cornelian cherry stone	46.44	5.99	0.26	47.13	0.18	1.43	[54]
Blackcurrent pomace	50.3	6.8	1.9	36.8	0.2	4.5	[41] [42]

Rice straw	36.81	5.025	-	56.69	-	-	[39]
Cconut fiber	47.75	5.61	0.9	45.51	0.23	8.1	[57]
Eucalyptus leaves	46.96	6.22	1.23	44.82	0.77	10.5	[57]
Litsea cubeba seed	59.6	9.3	1.7	15.4	-	6	[58]
Spent coffee	50.4	7.2	2.1	40.3	-	1.4	[59]
Barley straw	44.66	6.34	0.46	47.97	0.57	-	[40]
Corn stalk	39.24	4.92	0.81	42.52	0	-	[41]
Peanut vine	35.07	4.89	1.26	40.62	0	-	[41]
Hazelnut shell	52.9	5.6	1.4	42.7	-	1.4	[38]
Legume straw	42.52	6.05	2.71	48.6	-	6.4	[60]
Other Biomass							
Swine manure	41.1±0.2	5.42±0.09	3.36±0.1	50.1	-	16.3	[23]
Cattle manure	35.38	4.73	2.38	57.51	-	7.16	[61]
Mixtured Algal	27.9±2.6	3.01±0.5	3.900±0.4	65.2	-	47.5	[23]
Desmodesmus sp.	51.96	7.31	6.86	33.87	-	7.83	[62]
Spirulina platensis	46.87	6.98	10.75	34.86	0.54	-	[63]
Micro algal blooms	31.19	8.42	4.22	54.61	1.56	19.02	[64]
Dunaliella tertiolecta	39	5.37	1.99	53.02	-	13.54	[65]
Plastic waste	61.88	4.29	0.03	33.76	0.04	0.04	[66]
Microalgae (Chlorella p.)	46.8	6.8	8.4	17.2	-	9.1	[58]
Pulp/paper (Sludge powder)	45.6	5.2	7.2	25.3	1.7	15	[67]

2.5 Conversion of biomass to biofuels

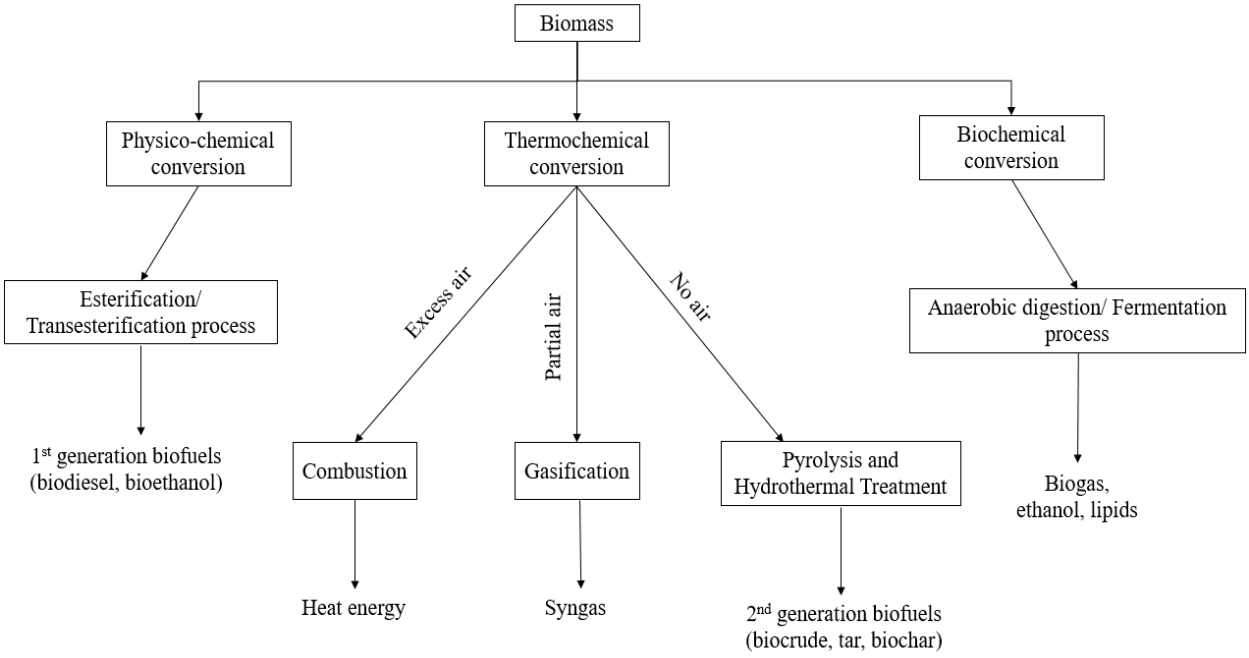

Figure 5 Different routes for the conversion of biomass to fuels/energy.

There are three major processing class available for production of fuels from biomass as described in Figure 5. The technology/route implemented for the conversion of biomass into energy and fuels depends significantly on few factors; firstly, the type of biomass available, secondly the properties of biomass feedstock, and finally the type of fuel/ energy required for use. For example, first-generation biomass such as sunflower oil and vegetable oil are already rich in fat and hence simple physico-chemical conversion process is enough for their conversion into first-generation biofuels. During combustion process in biomass based thermal plant for generation of heat, it is important that feed should be low in ash and high in heating value, therefore agricultural and forest feedstock is more viable than microalgae.

2.5.1 Physico-chemical route

The principle step and conversion route in physico-chemical process depends on the biomass feedstock. For first-generation biomass such as vegetable oils, cooking oils and animal fats conversion takes place by transesterification. In transesterification ethyl or methyl alcohol are used for conversion of fats into biodiesel in presence of alkaline catalyst [2, 29]. In case of lignocellulose biomass, the physico-chemical pretreatment is performed before implementing biochemical or thermochemical route of conversion. The physico-chemical pretreatment can be done by processes such as alkaline water treatment, hot water treatment, ammonia fiber explosion, steam explosion. The process of pretreatment alters biomass composition by solubilizing hemicellulose and/or lignin and decreasing the size of feed particles allowing more surface area for conversion process [69].

2.5.2 Biochemical route

The process of biochemical conversion can be routed into two directions; first, fermentation and second anaerobic digestion. Biochemical conversion is suited for herbaceous crops (corn cob, corn stover, wheat straw, barley straw, rice straw, sugar cane, bagasse, beet root), marine biomass(red, green, brown algae) and animal waste [70]. Alcoholic fermentation is used to produce high calorific value liquid fuels and gas, and anaerobic digestion is used to produce biogas.

In fermentation, sugar and starch crops are converted by enzymes into simple sugar which is subsequently converted to ethanol using yeast; for lignocellulosic biomass longer chain cellulose and hemicellulose molecules requires acid or enzymatic hydrolysis before fermentation step [71]. Anaerobic digestion is biochemical treatment of biomass by mixed culture microbes in the oxygen free environment. It is a four step process; hydrolysis: converting biomass into fatty acids, sugar

and amino acids, next, acidogenesis: breaking down hydrolysis products into more simpler compounds in presence of microorganisms, followed by, acetogenesis: employing microorganisms to convert acidogenesis phase products into acetic acid, CO_2 and H_2 and the final step is methanogenesis: methane is generated [13].

2.5.3 Thermochemical route

2.5.3.1 Combustion

Combustion is the process of conversion of fuel into heat energy in excess of oxygen. Biomass can be used as a fuel for combustion for production of energy in thermal power plant, factories, boilers etc. Biomass combustion consists of a series of complex heterogeneous and homogeneous reactions; main processes are drying, devolatilization, gasification, char combustion and gas phase oxidation [72]. For economical operation, combustion of biomass is feasible only for feedstock with less than 50% moisture content. The biomass combustion produces hot gases in temperature range of 800 – 1000 °C [71].

2.5.3.2 Pyrolysis

Pyrolysis of biomass is a fundamental thermochemical conversion process. In pyrolysis, conversion of biomass material takes places in the absence of oxygen. It is a promising route for the production of solid char, liquid tar and gaseous products [73]. The conventional pyrolysis route is called slow pyrolysis which takes place at lower temperature (350 – 550 °C), lower heating rates and greater residence time [48]; it is associated with majorly solid char production. At present the more favorable pyrolysis route is fast pyrolysis. In fast pyrolysis, biomass feedstock is rapidly heated to intermediate and/or high temperature range in absence of oxygen, with higher heating rate; it is mainly associated with liquid tar and gaseous fuel production [73].

2.5.3.3 Gasification

Gasification of biomass is the process of partial oxidation of feedstock at high temperatures, typically in the range of 800 – 900 °C. In first step of gasification, partial combustion of biomass occurs to produce char and gaseous mixture of CO_2, H_2O. The next step utilizes the produced char as catalyst for the reduction of H_2O into H_2 and CO_2 into CO. Other gaseous products such as methane and higher hydrocarbons are also produced depending on the design and operating condition of reactor [74].

2.5.3.4 Hydrothermal liquefaction

Hydrothermal liquefaction (HTL) is the process of thermochemical conversion of raw material in presence of solvent. Hydrothermal liquefaction is also known as hydrothermal treatment (HTT) and hydrothermal upgrading (HTU). In case of biomass it is treatment of biomass feedstock in liquid medium to produce energy dense fuels and high value chemical products. The most common medium used for HTL of biomass is water. Utilizing water as medium has two major benefits. First, use of water reduces the additional requirement for removal of inherent moisture from biomass, which can be a costly pre-treatment process with many other technologies such as pyrolysis, gasification and combustion. Second, presence of waster as medium in HTL facilitates the easy hydrolysis and degradation. It can be a batch or continuous process. The major parameters governing the process are temperature, pressure, retention time, feedstock, particle size, feed to water ratio, catalysts and reactor design. The process parameters are discussed in detail in Section 2.7.

2.6 HTL conversion process

Many researchers have carried out work in the field of HTL to increase the energy density of feedstock, to produce value added products, chemical and fuels. A summary of experimental setup, materials, condition, objective and results are provided in Table 4.

Table 4 (a) Summary of various HTL work, (b) objective and results

SN.	Biomass	Reactor	Media	Catalysts	Temperature, Pressure and Retention time	Ref.
1.	Sawdust	Autoclave batch reactor, 200 ml	Water (30 ml)	$Ca(OH)_2$ (0.0243M)	T: 180, 250, 280 °C RT: 15 and 60 min	[29]
2.	Pine wood (sawdust)	Autoclave batch reactor, 200ml	Water (30ml)	NaOH, Na_2CO_3, KOH, K_2CO_3 (0.94 M)	T: 280 °C RT: 15 min	[28]
3.	Wood (Konara)	Autoclave, stainless steel, 100ml	Water (30, 50, 80 ml)	K_2CO_3 (Various ratios)	T: 250 – 400 °C P: 0.5-10 MPa RT: 0, 30, 60 and 180 min	[75]
4.	Cornelian Cherry Stone	Batch SS Reactor, 500ml	Water (100 ml)	None	T: 200 ,250 and 300 °C RT: 0,15 and 30 min	[54]
5.	Empty palm fruit bunch (0.5-1.0mm)	Stainless steel Autoclave	Water (25 ml) Biomass (2.5-20 g)	KOH (0.1 M), NaOH (0.1 M), K_2CO_3 (0.1 to 2 M)	T: 270 °C P: 20 bars RT: 20min	[76]
6.	Microcrystalline cellulose	Conventional autoclave, 120cm^3	Water (30 ml)	Reduced Ni (2g in 30 ml), Alkali (0.2g in 30 ml)	T:200 – 350 °C P: 3 MPa RT: 0 min	[77]
7.	Barley straw (1.0mm)	High pressure Autoclave, 1000 ml	Water (150 ml)	K_2CO_3 (10 wt.%)	T: 280 – 400 °C RT: 0 min	[40]

8.	Sugar cane bagasse	Autoclave, SS, 200cm^3	Water (100 ml)	HCO_2Na, $Ca(OH)_2$	T: 140 – 350 °C RT: 15 min	[20]
9.	Waste biomass	Continuous one-step process, Fixed bed reactor	Water	ZrO_2 (pellets) Fixed bed catalytic rector, K_2CO_3 in feed stream	T: 330°C P: 25 MPa	[78]
10.	Litsea cubeba seed	Swagelok (1-in port and cap) SS batch reactor (25ml)	Water	Na_2CO_3 (0-10 wt.%)	T: 250 – 350 °C RT: 30 – 120 min	[58]
11.	Poplar wood	Parr 4848 autoclave 500 ml	Water (150 ml)	Lewis acids [$In(ITf)_3$, $Yb(OTf)_3$ and $InCl_3$] (0.5-10 wt.%)	T: 250, 275, 300 and 350°C P: 0, 1.0, 2.0 and 4.0 MPa RT: 5,10 and 20 min	[79]
12.	De-ashed microcrystalline cellulose	Batch reactor 9.7×10^{-5} m^3 Hastelloy C-22	Water (69.3 g)		T: 170 – 280 °C, P: 1 MPa, RT: 0 min Heating rate:0.0167 - 0.1667 Ks^{-1}	[47]
13.	Pulp/paper mill sludge + Newspaper Solid conc. (11.3 wt.%)	Parr autoclave reactor, 75 ml Hastelloy alloy	Sludge + newspaper water slurry	KOH (2-10 wt.%), FeS (5 wt.%), HCO_2H (5 wt.%)	T: 250 – 380 °C P: 2 MPa Rt: 20 min	[80]
14.	Cellulose (Cotton linter and dissolving softwood pulp)	Batch type reaction vessel, 5 ml Inconel-625	Methanol	None	T: 220 – 450 °C P: 14 - 72 MPa RT: 0.5 - 30 min	[81]
15.	Dairy manure	Autoclave 300 ml SS	Water (80 ml)	Na_2CO_3 (0 to 4 g)	T: 250 – 350 °C P: 2.068 MPa RT: 15 min	[82]

SN.	Objective	Products/Results &Conclusions	Ref.
1.	• Low- Temperature HTT study of biomass. • Effect of reaction parameters on products. • Effect of $Ca(OH)_2$ on biomass conversion and end products.	• Oil yield increases with temperature in given range of 180-280 °C, with maximum of 8.3 wt.% at 280 °C for 15 min. • For $Ca(OH)_2$ oil yield was 9.3 wt.% at 280 °C. • Hydrocarbons obtained were mostly being phenolic in nature.	[29]
2.	• Effect of Na and K hydroxides and carbonates on oil production from biomass from both solid and liquid extracts.	• Catalytic activity order K_2CO_3 > KOH > Na_2CO_3 > NaOH for bio-oil production. • Oil yield increased from 8.6 wt.% in water to 33.7 wt.% in presence of K_2CO_3. • Boiling point of hydrocarbons ranges near n-C_{11} and mainly phenolic in nature.	[28]
3.	• Effect of Pressure, Temperature, Holding Time and Wood/Catalyst/Water ratio on oil yield	• Argon pressure of 2 MPa, temperature 300 °C, holding time 0 min and catalyst concentration of 4-5 % was found to be preferable for high oil yield. • Oil yield of up to 47 wt.% was obtained.	[75]
4.	• To understand the effect of different reaction condition on HTT of cornelian cherry stones and bio-oil composition.	• Maximum bio-oil was obtained at 250 and 300 °C for zero residence time. • Total solid residue decreased as temperature increased for 200 to 300 °C. • Major compounds obtained were furfural and phenol derivatives in light oil, and in heavy oil it was majorly -oic acid and phenol derivatives.	[54]
5.	• Study of effect of different catalysts and catalyst concentration. • Study of biomass to water ratio to improve product yield and lignin degradation.	• 1.0 M K_2CO_3 yielded maximum conversion, while re-polymerization of biomass occurred on further increasing the catalyst concentration. • Major compounds obtained were phenolic and methyl ester groups. Phenolic group were absent in non-alkali runs.	[76]

6.	• To study the cellulose decomposition in hot compressed water under influence of alkali and nickel catalyst. • To understand the major reaction mechanism behind liquefaction and gasification of biomass.	• The cellulose decomposition occurs quickly between 240-270 °C and no cellulose remains after 280 °C in catalyst free condition. • In case of alkali cellulose decomposition started below 180 °C and gain pace between 260 – 300 °C. • In case of nickel as catalyst, cellulose decomposition started only after 260 °C. Nickel promotes catalysis of the aqueous products to gases.	[77]
7.	• To assess the practicability of converting barley straw to an alternative biofuel using HTL. • To understand product distribution obtained using HTL with and without aqueous phase recirculation.	• Low temperature bio-crude oil formation with maximum yield of 34.9 wt.% at 300 °C. • Major compounds were phenolic, carboxylic acids, aldehydes and alcohols. • Recycling of aqueous phase enhanced bio-crude yield with same property and facilitated higher carbon content in case of solid residue. • At low temperatures: Phenolic, carboxylic acids, aldehydes and alcohols. • Presence of aromatic compounds such as: benzene, fluorine and some alkenes at supercritical case.	[40]
8.	• To perform liquefaction of sugar cane bagasse with base/CO and formate/inert gas system.	• The heavy oil was highly oxygenated and solidified in air. • As a byproduct water soluble, unextractable carboxylic acids were formed.	[20]
9.	• To produce liquid biofuels from wet organic waste matter in a continuous one-step catalytic process.	• A reaction temperature of 330 °C, and pressure of 25 MPa was obtained to be appropriate. • Yield of n-C_7 and n-C_8 and the yield of n-C_{11} increased with alkali concentration.	[78]

10.	• To study the effect of temperature, time, reactor loading and catalyst loading on HTL of Litsea cubeba seed.	• Bio-oil yield of 56.9 wt.% was achieved at 290 °C, 60 min and reactor loading of 2.5 g with HHV of 40.8 MJ/kg. • Na_2CO_3 favored conversion but decreased bio-oil yield. • The bio-oil was mainly composed of fatty acid derivatives and phenyl derivatives.	[58]
11.	• To understand the effect of water tolerant Lewis acids on bio-oil and solid yield in HTL of Lignocellulosic material.	• The water tolerant Lewis acids had negative effect on bio-oil yields. • No change in molecular or elemental composition of products occurred due to catalysts.	[79]
12.	• Understanding the effect of heating rate on the liquefaction of cellulose. • Understanding concentration profiles of products using a theoretical model considering temperature profile during the reaction.	• A reasonable experimental fit was obtained. • For same final temperature of liquefaction, the amount of cellulose decomposition increased with decreasing heating rate. • The observation showed that it is necessary to consider heating effect when the rate of heating is below 1 Ks^{-1}.	[47]
13.	• To study co-liquefaction of pulp/paper mill sludge with waste newspaper, with and without catalyst over a range of temperature.	• Heavy oil yield without catalyst ranged between 16.7 to 28.0 wt.% and with 5 wt.% catalyst it increased to 24.9 to 34.4 wt.%. • Synergistic effect between pulp/paper mill sludge and newspaper waste was observed.	[80]
14.	• Study the chemical conversion of cellulose in supercritical methanol. • To study the kinetics of decomposition of cellulose.	• The main products from cellulose decomposition were methylated cellotriose, methylated cellobiose, methyl α and β-D-glucosides, levoglucosan and 5-hydroxymethylfurfural.	[81]
15.	• Testing bench scale HTL system for liquefaction of dairy manure to study bio-oil production and waste treatment.	• The higher heating value of acetone soluble fraction increased with temperature. • Maximum acetone soluble fraction was obtained at 350 °C when 1 g of catalyst was used and at same condition fraction of phenolic compounds was highest.	[82]

2.7 Operation parameters for HTL

2.7.1 Temperature

Temperature plays most crucial role to determine the progress of reactions during HTL. It helps in increasing hydrolysis rate for hemicellulose and lignin and promotes fragmentation and degradation of lignocellulosic biomass. The main role of temperature is to overshoot the energy barrier by providing enough energy for breaking of bonds. The initial rise in temperature gives rise to absorption of energy for bond breaking making HTL an endothermic process. During this step, large number of free radicals and fragmented compounds are produced. On further increasing temperature the exited radicals helps in repolymerization by formation of new bonds and release of energy making HTL exothermic in nature [83]. In general, the optimum range of HTL lies in between 250-375 °C. Hydrothermal liquefaction of biomass feedstocks has been studied in the temperature range of 180 – 400 °C [29], [54], [63], [84], with mid temperature range of 250 – 350 °C [40], [58], [63], [75], [82] and higher temperature range of 300 – 400 °C [40], [63], [75] [62].

The optimum temperature depends on the type of feed and the product of interest. Gan et al. [85], conducted a series of experiment on HTL of corn cobs and obtained optimized yield of different products. The highest yield of biooil was obtained at 305 °C, whereas the highest yield of solid char was found to be at 350 °C.

At lower temperatures (≤275 ºC), due to the partial breakdown of biomass the yield of product is low. It is also support by Minowa et al. [46]. He studied decomposition process of cellulose in hot compressed water and observed that there was quick decomposition of cellulose in 240 – 270 °C with all the cellulose decomposed near 280 °C. The products obtained before 240 °C were all water soluble products such as glucose; non-water soluble products such as oil, gas and char started to form after 240 °C.

Zhu et al. [40] conducted HTL of barley straw in temperature range of 280 – 400 °C with K_2CO_3 as catalyst. The results indicated no significant change in the product fraction in temperature range of 280 – 320 °C as low temperatures favors for ionic reactions involving hydrolysis and dehydration resulting in formation of intermediate products. The maximum yield of bio-oil was 34.9 wt. % at 300 °C and the biooil yield decreased to 19.9 wt.% at 400 °C. Zhu et al. [40] also indicated a decrease in oil yield and an increase in solid char yield as temperature increased from 320 – 400 °C. Similar decrease in oil yield above a threshold temperature is also indicated in many cited articles. The main reason for decrease in bio-oil yield with increase in temperature is concluded to be both; i) due to cracking and decomposition of oil in gaseous products and ii) repolymerization (carbonization) of bio-oil into higher molecular weight compounds resulting in increasing the bio-char percentage [29][28][75][77][40]. The results are also supported by GC-MS analysis of bio-oil indicating decrease in fraction of phenolic compounds with increase in temperature due to polymerization of phenolic compounds into higher molecular compounds leading to formation of solid char [40]. However, Minowa et al. [77] also indicated in the developed reaction methodology that presence of alkali as catalyst decrease the repolymerization of bio-oil to char.

Karagoz et al. [29] observed that with increase in temperature from 180 – 280 °C total conversion increased from 26.7 wt.% to 58 wt.% and oil yield increased from 3.7 wt.% to 8.5 wt.%. Ogi et al. [75] suggested that 300 °C to be the most ideal temperature for HTT of wood for higher yield, though as high as 375 °C can be used to obtain low viscous oil. Hence, a generic reasoning would be that biooil yield increases with increasing temperature to a threshold limit, after that it starts to repolymerize to form solid resulting in decrease of oil yield.

The GC-MS results obtained by Kurse et al. [86] for liquid fuels indicated an increase in the phenol and cresol fraction on increasing temperature from 330 – 370 °C and then a decrease on further increase in temperature; while the lumped concentration of total phenol derivatives decreased with temperature. The C-NP curve obtained from GC-MS data in Karagoz et al. [28] suggested that majority of compounds present in oil lies near C_{11}. As listed by Zhu et al. [40] for HTL in subcritical temperature range major compounds were phenolic in nature along with 25 % of short chain, long chain and aromatic acid derivatives while in supercritical temperature range the percentage of acid compounds decreased to 15 % due to breakdown of acids into CH_4 and CO_2 while there was some presence of aromatics and alkenes such as benzene, fluorene and 3-ethyl-2-methyl-1,3-hexadiene. Kurse et al. [86], conducted biomass conversion in water at 330 – 410 °C and observed an increase in the carbon content in the gas phase which was mainly due to CO_2 produced from gasification. A steady increase in other hydrocarbons in gas such as ethane, ethene, propane, propene, isobutane, methyl propene, butene was also observed with increasing temperature.

2.7.2 Pressure

Hydrothermal experiments are carried out in an inert medium. In general, nitrogen is used as medium gas in the reactor. Reactor pressure is also an important parameter that governs the path of HTL process of biomass. The initial pressure maintained in reactor is decided based on the extent of vapor phase formation during operation. Pressure reduces phase change of water from liquid to vapor during liquefaction at all given temperature range; hence reducing the need of additional energy required in a two-phase system to maintain operation temperature [87].

Yang et al. [59] conducted HTL for spent coffee ground as feedstock; the two main outcomes observed were: the change in initial pressure form 0.5 MPa to 2 MPa at 275 °C has little

effect on the yield of bio-oil, second the final pressure reached to 6.0 MPa indicating phase change of water. It was also observed that at lower initial pressure it took longer time to reach final temperature; indicating an increased energy requirement to maintain temperature in two-phase system. The result of studies by Ogi et al. [75], also discusses the effect of pressure on direct liquefaction of wood, in which it was observed that oil yield varies significantly from 5.92 wt.% to 20.1 wt.% on increasing pressure from 0.5 to 4.0 MPa at 350 °C. Akhtar et al. [83], concluded that pressure has negligible effect on yield of oil and gas once critical condition of water is reached; this is because effect of pressure on water properties is minutia in supercritical region and the increase in local solvent density causes cage effect inhibiting C – C bond cleavage.

Kurse et al. [86] concluded that pressure dependency of gaseous products come into play only after critical point of water; it was observed that H_2 and CO_2 decreased with increasing pressure whereas composition of C_2, C_3 and C_4 compounds increased. In addition, the fraction of phenols in liquid fuels was observed to increase on increasing pressure from 30 – 50 MPa.

2.7.3 Retention time

Retention time affects the total conversion, biooil, solid char and gas phase yield. Retention time is defined as the total time for which the reactor is maintained at final temperature once it reaches there, it doesn't account for the overall heating and the cooling period. The effect of retention time greatly depends on the type of feedstock and its composition.

Karagoz et al. [29], conducted retention time experiment on sawdust HTL for production of bio-oil and obtained an increase in yield of oil from 3.7 wt.% to 5.3 wt.% on increasing retention time from 15 to 60 min at lower temperature of 180 °C. On increasing the retention by same time at higher temperature of 280 °C it was observed that oil yield decreased from 8.5 wt.% to 6.6 wt.%. In an investigation on HTL of blackcurrent pomace presented in Deniel et al. [56], retention time

of 0 to 240 min was studied at fixed temperature of 573 °C; the results suggested that majority of the reactions were completed before the start of retention period and the retention period had no major effect on overall yield of products, though the yield of the bio-oil decreased during the first 15 min of retention time. Gao et al. [88], performed retention time experiment from 5 min to 120 min on HTL of cellulose and obtained that shorter retention time promotes cellulose hydrolysis and inhibits further decomposition promoting bio-oil formation; maximum yield of oil was at retention time of 10 min and no significant change on yield of bio-oil was observed from 10 to 120 min retention time.

Akalin et al. [54] presented an elemental composition of biofuels produced at different temperature and observed that for heavy oil and aqueous oil phase of bio-oil on increasing retention time from 0 to 30 min at constant temperature, the total carbon wt.% and higher heating value increased. In case of solid char, the results were opposite as the carbon wt.% and higher heating value decreased with increase in retention time.

Hence, it can be summed up that lignocellulosic biomass decomposes during heating cycle and increased retention time has little effect on yield; the composition of biooil improves for longer retention time as carbon wt.% increases, whereas the carbon wt.% in char decreases with retention time. Due the fact that conversion of biomass into bio-oil takes place at shorter retention time, the use of continuous HTL unit becomes more viable and economic.

2.7.4 Feed to solvent ratio

In general, water is used as the solvent in HTL. Wang et al. [89] conducted a series of experiments using different supercritical solvents such as carbon dioxide, water, acetone and ethanol. The oil yield was maximum with ethanol as solvent whereas minimum with water. The order of yield with different organic solvent was ethanol (30.8 wt.%) > supercritical carbon-di-

oxide (29.3 wt.%) > acetone (27.9 wt.%) > water (17.3 wt.%). Cheng et al. [27], observed utilizing 50% co-solvent either alcohol (methanol, ethanol)-water to be most effective solvent for HTL than 100% alcohol or water. The results presented synergistic effect of alcohol-water co-solvents on lignocellulosic biomass, as hot-compressed water carries hydrolysis of polymer structures in biomass and alcohol reduces surface tension of liquid products making it more penetrable in lignin matrix. Furthermore, alcohol helps to dissolve high molecular compounds derived from cellulose and hemicellulose because of low dielectric constant than water. Li et al. [39] performed liquefaction of rice straw in sub and supercritical 1,4-dioxane-water and observed a significant oil yield increase in case when 1,4-dioxane to water ratio was (1:1 and 4:1) in comparison to pure water run. The presence of 1, 4-dioxane helps to solubilize the cellulose and hemicellulose and carries the fragmented lignin from the inner part of the plant tissue to the solution.

2.7.5 Catalyst

Catalysts play a very promising role to decide the reaction pathway, formation and quality of products. The main objective to use catalyst is to direct the process specific towards production of fuel in interest. Several catalysts had been tested for HTL of biomass. The two major class of catalysts are the homogeneous and the heterogeneous catalysts. Homogeneous catalysts are considered to be very effective in the process of liquefaction of lignocellulosic biomass. Some of the common homogeneous catalysts used in HTL are hydroxides and carbonates of alkali (Na, K) and alkaline earth metals (Ca) such as NaOH, KOH, Na_2CO_3, K_2CO_3, $Ca(OH)_2$ [23, 38, 42, 45, 48, 53]. Tekin et al. [90] reported the use of natural calcium borate mineral for the HTL of beech wood and observed that the total bio-oil yield increased at all condition; there was a significant increase in bio-oil with decrease in char yield in presence of catalyst at 300 °C. Minowa et al. [77], observed a decrease in char formation and more oil production in presence of alkali. Karagoz et

al. [9] and Akhtar et al. [76] conducted a series of experiments to understand the effect of different alkali hydroxides and carbonates and ranked them in the order K_2CO_3>KOH>Na_2CO_3>NaOH>H_2O. Xu et al. [92] studied the effect of iron-based catalyst and reported that it increases the total oil yield, with reduction in char and gas formation. Many other literatures have reported K_2CO_3 as the most effective catalyst for HTL [89]. Karagoz et al. [29], observed that for the same temperature and retention time condition of 280 °C and 15 min, the yield of bio-oil during HTL of sawdust increased 8.5 wt.% to 9.3 wt.% in presence of $Ca(OH)_2$ as catalyst.

Xu et al. [92] studied effect of FeS and $FeSO_4$ on liquefaction of woody biomass in sub/super-critical ethanol. It was observed that both catalysts enhanced the oil yield and suppressed the formation of gas, the catalytic activity became more visible on higher temperature as oil yield was observed to increase from 44 wt.% with no catalyst to 63 wt.% with 5 wt.% $FeSO_4$.

Chapter 3 : Experimental Methods

3.1 Feedstock preparation

The corn stover was collected from farms in southern and northern Alberta, Canada by large-scale fluid laboratory, Department of Mechanical Engineering, University of Alberta. The material was processed through various steps for cleaning and classification as mentioned in Vaezi et al. [93]. The feedstock received from the fluid laboratory was further segregated into different sizes to obtain a feed size range of 0.425 – 1 mm, which was used in HTL experiments.

Figure 6 Corn stover reduction from > 9mm to 0.425 – 1 mm

3.2 HTL experiments

Hydrothermal Liquefaction experiments were conducted in a 250 ml T-316 SS autoclave reactor (Parr Instruments) having upper limit pressure and temperature range of up to 5000 psi (34.47 MPa) and 500 °C, respectively. The reactor was equipped with a mechanical stirrer connected to an electric motor, cooling water circuit, thermocouple connected to a control box, pressure gauge and gas inlet and outlet line supported with Swagelok ball valve. The reactor vessel had an inner diameter of 6.4 cm and stirrer impeller had a diameter of 5.2 cm. The depth of reactor

vessel was 8.5 cm and stirrer was at a clearance of 0.5 cm from bottom of vessel. The material reached till a height of 1.5 – 2 cm giving stirrer enough contact for proper mixing.

Figure 7 In-lab HTL set-up with controller system

For an experiment, 5 g of as received corn stover and 30 ml of deionized water (Milli-Q® Gradient Instrument) was loaded into the reactor. The reactor was sealed with gasket, clamped and tightened with hexagonal screws. reactor was purged with nitrogen 3 times to remove the reactive species. In order to do leak test, reactor was pressurized to 300 psi and waited for 15 min. The reactor was then pressurized to an initial pressure (Pi) of 300 or 600 psi as per operation condition. A stirring speed of 75 revolution/ min was set. The total pressure inside the reactor varied throughout the reaction to reach a final pressure (P_f) in the range of 1100 to 3400 psi depending on initial pressure, temperature, amount of water (constant) and gaseous product formation. The reactor was heated to a target temperature of 250, 300, 350 and 375 °C as per heating cycle presented in Figure 8. The reaction was carried out for retention time of 0, 15, 30 and 60 min;

where 0 min corresponds to immediate start of cooling through chilled water circulation after temperature reaches set value. A schematic of the reactor setup is shown in Figure 9.

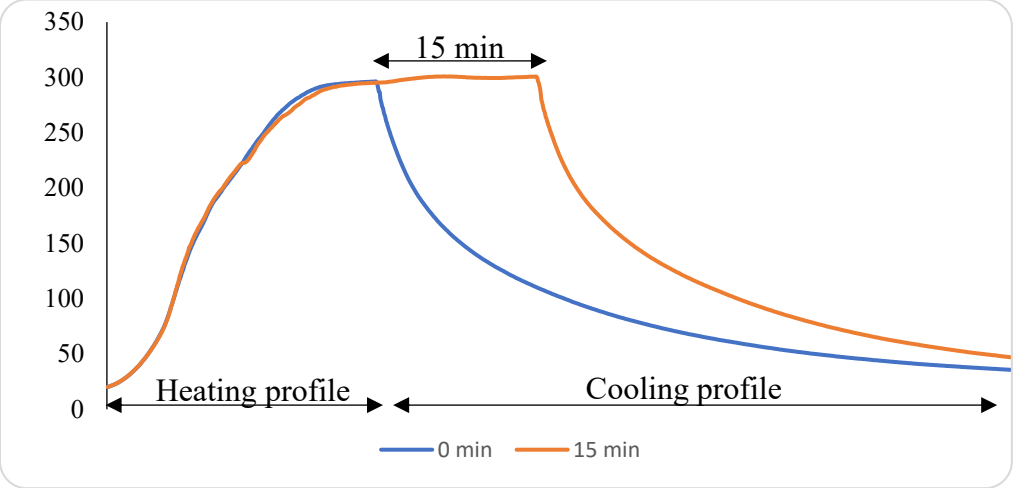

Figure 8 Heating and cooling cycle of the reactor for HTL at 300 °C for 0 and 15 min retention time

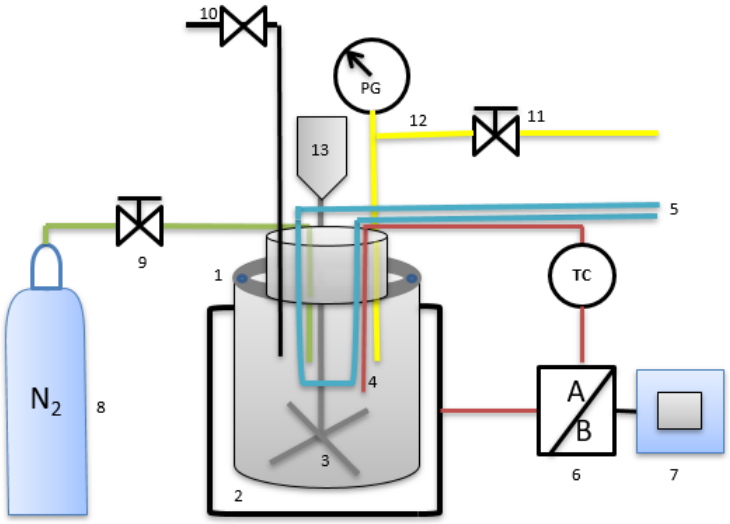

1. Autoclave Reactor
2. Furnace
3. Mechanical Stirrer
4. Thermocouple
5. Cooling Water Supply
6. Control Box
7. Computer
8. Gas Cylinder(N_2)
9. Gas Inlet Valve
10. Pressure Relieve Valve
11. Gas Outlet Valve
12. Pressure Gauge
13. Electric Motor

Figure 9 Schematic diagram of high temperature, high pressure autoclave reactor.

3.3 Product recovery and separation process

Once the heating and cooling cycle of the reactor was over, the reactor was depressurized, the gas samples were collected in Tedlar bags for analysis. Depressurized reactor was opened, and

the products were recovered and separated following the stepwise procedure described in Figure 10. The product content in the reactor was recovered using a spatula and filtered on Buchner funnel using Whatman filter paper in vacuum condition. The final solids in the mixture tend to stick to the surface of the reactor and stirrer at higher temperatures whereas it was found to be mixed in final slurry at lower temperatures. The filtered aqueous phase product was rotary evaporated to obtained aqueous phase oil (AO). The sticky residues at the bottom of the reactor were recovered through multiple acetone (Fisher Chemicals 99.5 % purity) wash. The acetone washed mixture recovered from the reactor and solid residue from the aqueous phase was again washed with additional acetone in order to extract all the oil such as oil trapped in inner side and pores. The complete acetone mixture was filtered. The insoluble fraction was dried at 70 °C for 1 hour and further kept at room temperature for 24 hours, the final solid residue was termed as hydrochar (HC). All the acetone from acetone phase was removed using rotary evaporation under vacuum condition. The resulting dark brown highly viscous liquid was termed as crude bio-oil or heavy oil (HO).

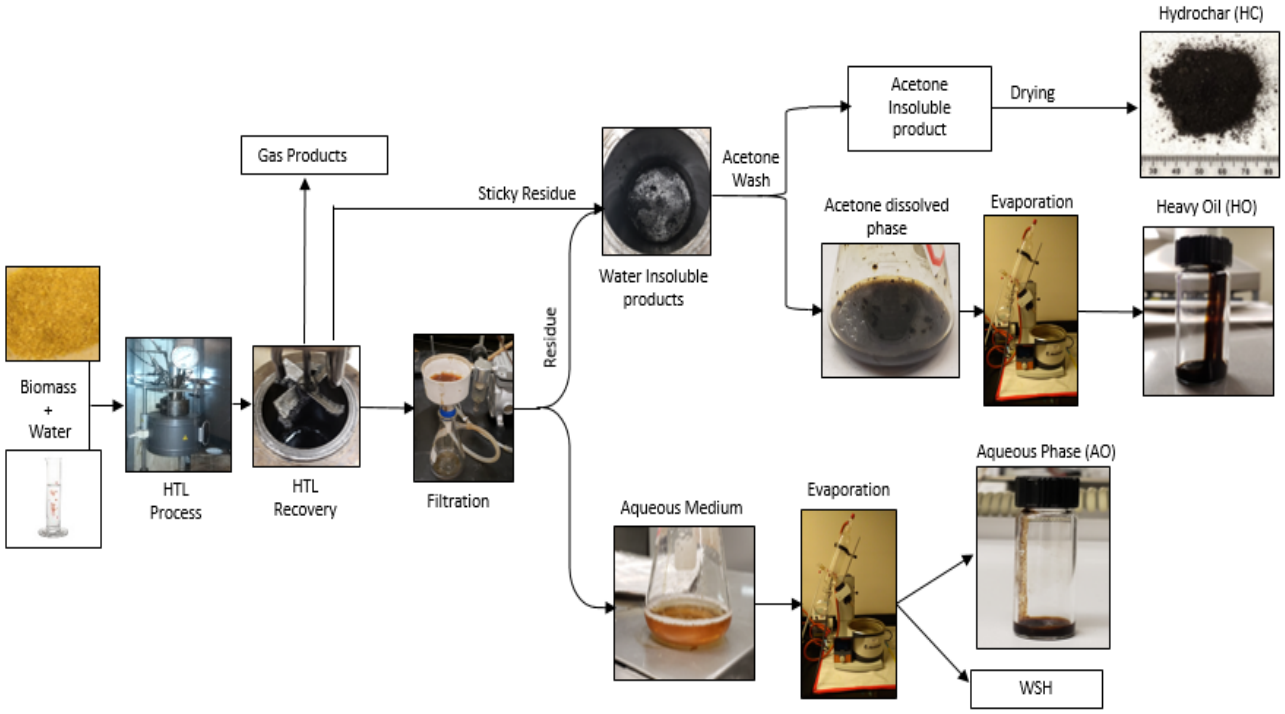

Figure 10 Product recovery and extraction procedure. Where; HTL: hydrothermal liquefaction; WSH: Water soluble hydrocarbons

3.4 Characterizations

3.4.1 Proximate analysis

After feed preparation, the corn stover of size 0.425 - 1.0 mm was used for proximate study. The moisture, volatile matters, ash content and fixed carbon in the feedstock were studied in LECO TGA 701 using ASTM D7582 method. Approximately 1 g of sample was taken in the ceramic crucibles. Initially, the samples were heated till 107 °C in nitrogen atmosphere until constant mass was achieved and the moisture content was obtained from the loss of mass in sample. The temperature is then increased till 900 °C at the rate of 40 °C min^{-1} with holding time 15 min in

nitrogen atmosphere to obtain volatiles and fixed carbon. Finally, the ash content was measured by lowering temperature to 500 °C followed by heating to 575±25 °C, in an oxygen atmosphere.

Figure 11 Proximate analysis: LECO TGA

3.4.2 Elemental analysis

The elemental composition (C, H, N, S, O) was determined using Thermo fisher flash 2000 organic elemental analyzer at Department of Chemistry, University of Alberta. The sample was enclosed in a tin cup and dropped in vertical quartz tube maintained at a temperature of 1000 °C with a constant flow of helium as a carrier gas. Once the sample is in combustion chamber a fixed volume of oxygen gas is mixed with helium for combustion of sample and tin cup. The individual gases are detected by thermal conductivity detector and the Eager Xperience software provides peaks for carbon, hydrogen, nitrogen and sulfur percentage. The oxygen weight percent is obtained

by difference. The HHV (higher heating value) was calculated using Dulong formula [HHV = 0.338*C+1.428*(H-O/8)+0.095*S].

Figure 12 Elemental analysis: Thermo fisher FLASH 2000

3.4.3 GC-MS analysis

The heavy oil composition was analyzed on Gas Chromatograph (Agilent Technologies 6890N) coupled with Mass Spectrometer (HP 5973 MSD) (GC-MS). The column used for the analysis was a 5 % Phenyl Methyl Siloxane capillary column 30 m × 0.25 mm, 0.25 µm film thickness. A small amount of HO was dissolved in dichloromethane as solvent. The mixture was micro-centrifuged, and the supernatant was used for analysis after filtration using 2-micron PTFE filter. For analysis, 1 µL of sample was injected in split mode (50:1) with Helium as a carrier gas.

The temperature profile for column heating in GC starts at 40 °C with a hold time of 5 min and next heating at ramp of 5 °C min^{-1} to reach 170 °C hold time 5 min and finally heating at same ramp up to 280 °C hold time 5 min. The temperature at auxiliary interface between GC and MS was maintained at 280 °C. Likely compounds in sample were identified using NIST library for mass spectra.

Figure 13 GC-MS analysis: GC (Agilent Technologies 6890N - MS (HP 5973 MSD)

3.4.4 FTIR

The raw corn stover feedstock and HC collected from the runs at different conditions of temperature, pressure and retention was analyzed to understand the presence of different functional groups. The Thermo NEXUS 870 FT-IR equipped with SMART DIFFUSE REFLECTANCE was used for analysis. The samples were finely crushed in a mortar crusher to pass it through 250 µm sieve. A small pinch of sample was mixed with potassium bromide and a smooth reflective sample disk was prepared on sample cup and it was tested to obtained transmittance vs wavenumber peak curve.

Figure 14 Diffuse Reflectance Thermo NEXUS 870 FTIR

3.4.5 SEM analysis

In order to understand surface morphology of hydrochar scanning electron microscopy was performed on Zeiss Sigma 300 VP-FESEM at Department of Earth and Atmospheric Sciences, University of Alberta. The sample prepared for FTIR was coated on the top of sample holder. Initial test suggested good results without any conductive coating, hence no coating was used to

improve the conductivity. Conductive carbon tape was used to ground the sample to the holder. For analysis, SEM scans were conducted at an accelerating voltage of 10 kV.

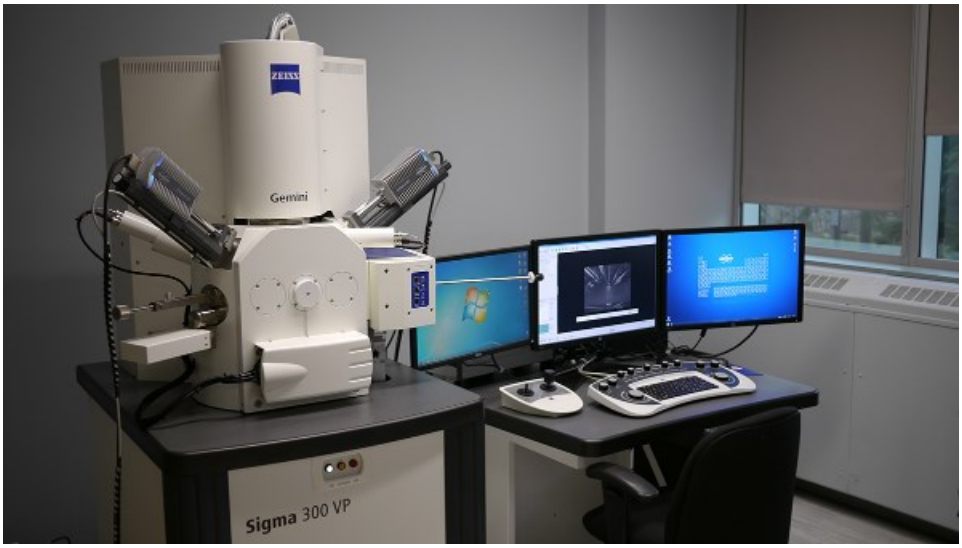

Figure 15 Scanning Electron Microscope Zeiss Sigma 300 VP-FESEM

3.4.6 BET study

Brunauer-Emmett-Teller (BET) experiments were performed to obtain the surface area of the hydrochar on an Autosorb IQ instrument (Quantachrome Instruments, Boynton Beach, FL, U.S.A.). For BET experiments, 9 mm cells were filled with sample till 3/4th of cell (bulb) volume. The sample were degassed by heating sample in vacuum at 250 °C at heating rate of 5 °C min^{-1} and the soak time was 4 hours. The adsorption and desorption isotherm of nitrogen was measured at a relative pressure range of 0 - .99 at 77 K. The multipoint BET surface areas were measured at a relative pressure range of 0.05–0.30.

Figure 16 BET set-up, Quantachrome IQ

Chapter 4 : Results and Discussions

4.1 Feed characterization

After classification of feedstock to 0.425 – 1 mm size; proximate analysis and elemental analysis (CHNS) were performed. The moisture, volatile matters, ash content and fixed carbon in the feedstock were determined by LECO TGA 701 using ASTM D7582 method. Approximately 1 gm of sample was taken in the ceramic crucibles. Initially, the samples were heated to 107 °C in nitrogen atmosphere until constant mass was achieved and the moisture content was obtained from the loss of mass in sample. The temperature is then increased to 900 °C at the rate of 40 °C min^{-1} with holding time 15 min in nitrogen atmosphere to obtain volatiles and fixed carbon. Finally, the ash content was measured by lowering temperature to 500 °C followed by heating to 575±25 °C, in an oxygen atmosphere. The elemental composition (C, H, N, S, O) was determined by using Thermo fisher flash 2000 organic elemental analyzer at Department of Chemistry, University of Alberta. The Higher Heating Value (HHV) was calculated using Dulong formula. The ICP-MS (Perkin Elmer Elan 6000 quadrupole) analysis were conducted to determine the metals content in the feedstock at Canadian Centre for Isotopic Microanalysis, University of Alberta. All experiments were performed in triplets for accuracy.

Table 5 Proximate, elemental and selected metals content in corn stover

Proximate Analysis	**Moisture**	**Volatiles**	**Ash**	**Fixed Carbon**
	5.41	70.96	6.96	16.77

Elemental Analysis	**C**	**H**	**N**	**S**	**O**[1]	**H/C**	**O/C**	**N/C**	**HHV**[2]
	43.57	5.84	0.56	0.05	49.98	1.61	0.86	0.011	14.14

Selected Metals	**Na**	**Mg**	**Al**	**P**	**K**	**Ca**	**Fe**
	144	1282	205	422	12588	1731	239

[1] Oxygen wt. % by difference = 100-[(C+H+N+S) wt. %]
[2] Higher Heating Value was calculated by the Dulong formula, i.e., HHV = 0.338*C + 1.428*(H-O/8) + 0.095*S

4.2 Product distribution

The experimental results were summarized to understand the effect of temperature, pressure and retention time. For all the experiments the feedstock to de-ionized water ratio was kept constant (1:6) i.e., 5 g of (0.425 – 1 mm) corn stover and 30 mL of de-ionized water. The ratio of feed and the size of feedstock were fixed after some preliminary experiments and literature review. The design of the reactor was best suited for feed ratio of 1:6; increasing concentration of feed tends to cease the stirrer and at higher water fraction the final pressure tends to cross the manufacturing limit of pressure for reactor. Furthermore, Ogi et al. [75] and Karagoz et al. [29] supports use of the considered feed ratio. In order to determine the suitable size of feedstock three size range of feedstock <0.425 mm, 0.425 – 1 mm and 1 – 2 mm were used. Experimental runs were conducted with each size of feedstock at temperature, initial pressure and retention time condition of 300 °C, 600 psi and 15 min. After these preliminary runs it was observed that the feedstock with size greater than 1mm had unconverted material left in the products, whereas the feedstock with size range <0.425 mm tends to produce more hydrochar and increases the turbidity in the aqueous phase. Hence, feedstock with size 0.425 – 1 mm was observed to match best with experimental requirements.

The yield of different products is presented in Table 6. The major products are HC, oil phase and gas. The oil phase is composed of AO and HO. The HO was considered as the significant fraction of oil based on characterization results whereas AO was considered as side products due to its low HHV value. Hence, in majority of the analysis and comparison emphasis is given on HO.

Table 6 Product Distribution at different condition of temperature, pressure and retention time

T(°C)| RT(min)	P_{intial}/ P_{final} (psi)	HC wt.%	Conversion wt.%	Oil Phase		Gas wt.%	WSH wt.%
				AO wt.%	HO wt.%		
250|15	300/1100	23.5	76.5	13.5	19.35	12.29	31.36
300|15	300/1650	23.4	76.6	10.2	21.75	14.44	30.21
350|15	300/2600	30.21	69.79	9	17.7	10.74	32.35
375|15	300/2850	25.52	74.48	8.55	14.25	13.5	38.18
250|15	600/1600	22.29	77.71	15.6	22.2	12.89	27.02
300|15	600/2200	21.41	78.59	13	27.15	9.58	28.86
350|15	600/3150	26.84	73.16	9	17.7	11.2	35.26
375|15	600/3500	22.44	77.56	6.66	14.25	18.07	38.58
300|0	600/2200	17.38	82.62	13.36	29.25	10.67	29.34
300|30	600/2200	20.02	79.98	10.5	25.2	17.37	26.91
300|60	600/2200	19.36	80.64	8.1	23.55	17.54	31.45

Where, HC: Hydrochar, WSH: Water soluble hydrocarbons, 250|15: set temperature 250 °C and retention time 15 min, 300/1100: initial pressure: 300 psi and final pressure 1100 psi

$$Conversion\ wt.\% = \frac{W_{CS}-W_{HC}}{W_{CS}} * 100$$

$$Aqueous\ oil\ wt.\% = \frac{W_{AO}}{W_{CS}} * 100$$

$$Heavy\ oil\ wt.\% = \frac{W_{HO}}{W_{CS}} * 100$$

$$Hydrochar\ wt.\% = \frac{W_{HC}}{W_{CS}} * 100$$

$$Gas\ wt.\% = \frac{W_F-W_R}{W_F} * 100$$

$$WSH\ wt.\% = 100 - (W_{HC} + W_{AO} + + W_{HO} + W_{Gas})$$

$$W_F = Weight\ of\ feed\ (corn\ stover + deionized\ water)$$

$$W_R = Weight\ recovered\ from\ reactor$$

Quantitative analysis of the result presented in Table 6 shows that at 300 °C, 600 psi and 0 min, highest conversion of 82.62 wt.% was observed. At the same condition maximum amount of

HO 29.25 wt. % was obtained. HC was maximum at 350 °C, 300 psi and 15 min with 30.21 wt. %. Gaseous products were highest for supercritical condition (375 °C) of water and at longer retention time (60 min).

4.2.1 Effect of temperature

The temperature plays an important role during HTL with respect to the products quantity and quality. Each product can have its specific optimum temperature condition. In order to understand the effect of temperature a series of experiments were conducted for a feed ratio of 1:6 and retention time of 15 min. The temperatures analyzed were 250, 300, 350 and 375 °C on initial pressure of 300 psi and 600 psi.

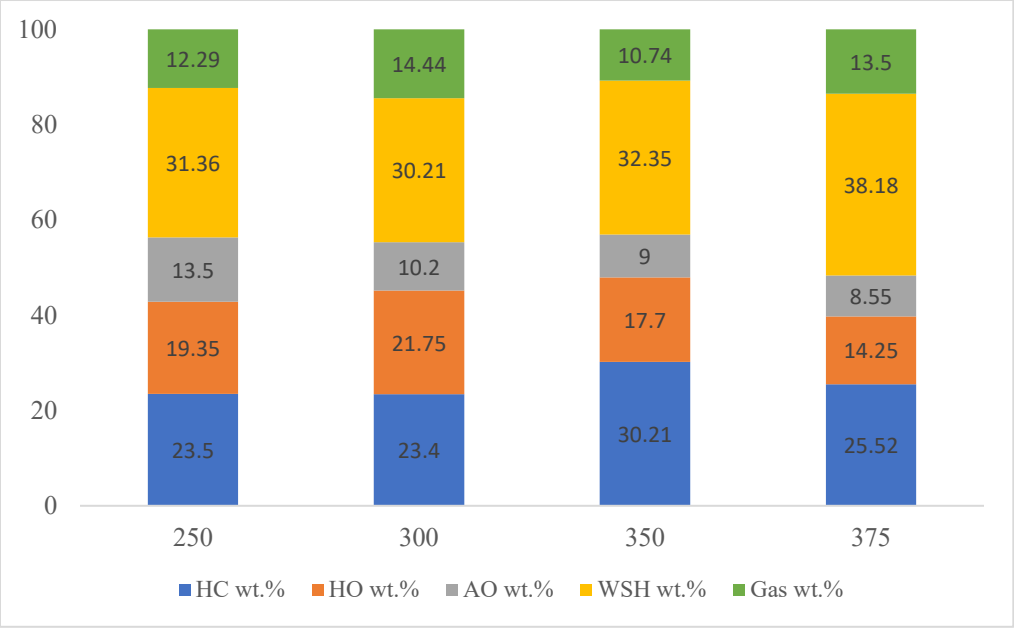

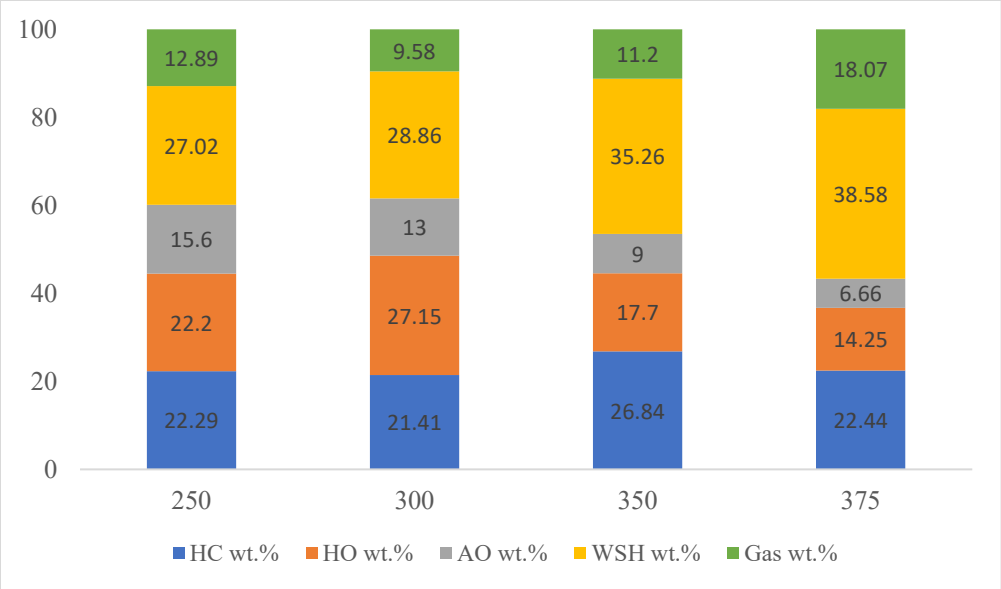

Figure 17 Product fraction variation with temperature at retention time of 15 min and pressure a) 300 psi, b) 600 psi

In the selected temperature range, HO ranged between 14.25 - 21.75 wt.% and HC ranged between 23.4 - 30.21 wt.% for initial pressure of 300 psi and retention time of 15 min. For the same temperature range and retention time but with initial pressure of 600 psi HO varied between 14.25 - 27.15 wt.% and HC wt.% varied between 21.41 - 26.84 wt.%.

As shown in Figure 17, it was observed that initially with increase in temperature from 250 to 300 °C HO weight percentage increased but at the same time HC wt. % varied a little. The yield of oil was maximum at 300 °C which is comparable to the other studies on HTL of agricultural and forest feeds [15, 39, 53]. On increasing temperature above 300 °C till 375 °C both AO and HO wt.% kept on decreasing. Similar trends have been depicted by many other researchers. Initially, in the temperature range of 300 to 350 °C the total HC wt. % increased significantly leading to a steep drop in HO wt. %. One possible reason for this observation is due to

carbonization of intermediate compounds from HO to form HC [39, 53]. In the second half when temperature increased from 350 to 375 °C it can be observed that both HO and HC wt.% decreased with a peak increment in total gas wt.%. This indicates that there has been cracking of HO into gaseous products.

Hydrolysis and dehydration favor ionic reaction at low temperature. First ionization of biomass gives rise to monomers in the polar medium. With increase in temperature and based on composition of biomass decomposition of hemicellulose, cellulose and lignin takes place [83]. The highest amount of AO i.e. 13.5 wt.% and 15.6 wt.% was observed at 250 °C for an initial pressure of 300 and 600 psi at retention time of 15 min, respectively. This increased amount of AO percent was most probably because of linking of increased WSH products which concentrated due to sudden rise in hemicellulose and cellulose decomposition [29]. The increased decomposition produces highly water-soluble products, as discussed in Minowa et al. [46], cellulose decomposes rapidly near 250 °C and no cellulose was left above 280 °C. On increasing temperature above 300 °C, two simultaneous reactions i.e. repolymerization of oil to form HC and depolymerization of oil and HC occurs to form gaseous products [11, 39]. In temperature range from 300 to 350 °C, it can be said that the first reaction of HC formation dominates, as total HC wt. % increased from 23.4 wt.% at 300 °C to 30.21 wt.% at 350 °C and also from 21.41 wt.% at 300 °C to 26.84 wt.% at 350 °C for retention time of 15 min and initial pressure of 300 and 600 psi, respectively. Based on experimental results the probable reason for this increase might be from repolymerization of oil, as HO content decreased rapidly. Further, increase of temperature above 350 °C initiates cracking of HO and HC resulting in increase of the gaseous products and WSH [11, 39]. As observed at 600 psi and retention time of 15 min, the total gaseous products increased by 60 % on increasing temperature to 375 °C from 350 °C whereas the oil and HC were decreased. Ogi et al.

[75] indicated that heavy oil obtained at temperature other that 375 °C tends to solidify in atmospheric condition whereas at 375 °C its possess less viscosity, similar phenomena was observed with heavy oil obtain from corn stover liquefaction in these experiments at 350 and 375 °C.

4.2.2 Effect of pressure

Reactor pressure is also an important parameter that governs the path of HTL process of biomass. In order to understand the effect of pressure the experiments were performed at two different initial pressures 300 and 600 psi. In this study, reactor limits on increasing initial pressure above 600 psi as the final pressure tends to cross the maximum working pressure suggested by the manufacturer. Furthermore, Ogi et al. [75] and Yang et al. [59] have reported the similar pressure range for HTL experiments as optimum and effective.

Effect of pressure on HO yield was more obvious at lower temperature of 250 – 300 °C whereas it had no effect at higher temperature of 350 – 375 °C. At supercritical condition of water (374 °C and 3200 psi) pressure had negligible effect on HO yield. This could be because in supercritical region pressure has limited effect on properties of water; and the increase in local solvent density causes cage effect inhibiting C – C bond cleavage [83].

On increasing pressure from 300 to 600 psi, yield of AO and HO increased whereas HC wt.% decreased for all considered temperatures. The HO fraction increased significantly by 24.8 % for 300 °C, 15 min. The observation is also supported by earlier publications [23, 53]. Both the temperature and pressure study concluded to take 300 °C and 600 psi as ideal condition to study retention time study.

4.2.3 Effect of retention time

Retention time is the time period during which the reactor is held at the desired final temperature before initiating cooling cycle, as shown in Figure 1. Retention time of 0, 15, 30 and 60 min was studied at 300 °C and P_i of 600 psi. During HTL, rate of hydrolysis and degradation is comparatively fast, it has been observed shorter retention time yields higher oil fraction [23, 24, 53]. Majority of the reaction reach to its extent during long heating cycle of the reactor to achieve the final temperature as shown in Figure 8.

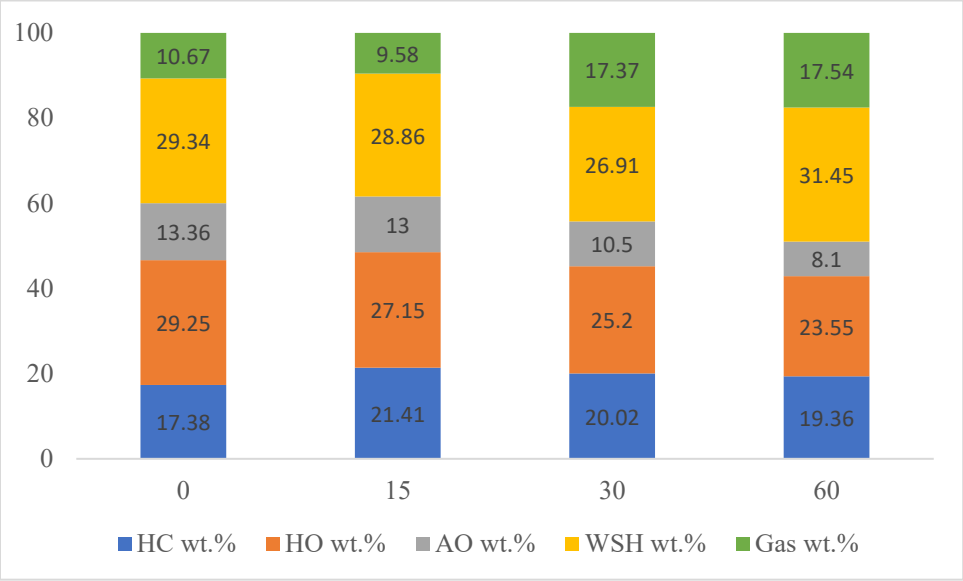

Figure 18 Product fraction variation with time at 300 °C and 600 psi

With increase in time from 0 to 15 min HO, AO and gas fraction decreased, and HC content increased as shown in Figure 5 suggesting carbonization reaction in oil. On further increasing time from 15 min, HO and HC wt. % started to decrease and gaseous fraction increased significantly. It could be said that at longer retention time decomposition of oil and char was promoted. The results indicating higher oil yield at 0 min retention time supports for possibility to carry out experiment in continuous flow reactor.

4.3 Product analysis

In previous section, a quantitative classification of products was carried out. This section aims at qualitative analysis of various products obtained during HTL.

4.3.1 Elemental analysis, atomic ratio and HHV

Both char and oil phase are composed of majorly carbon, hydrogen, nitrogen and oxygen. Oxygen percent is calculated by difference, whereas sulphur was lower than detection limits. HHV value was calculated using Dulong formula as discussed in section 3.4.2.

4.3.1.1 Hydrochar

Table 7 Elemental composition and HHV value for hydrochar samples produced at different conditions

Hydrochar	C	H	N	O	H/C	O/C	N/C	HHV (MJ/kg)
HC(300, 300, 15)	66.58	4.81	2.15	26.46	0.87	0.3	0.028	24.65
HC(250, 600, 15)	60.72	4.42	2.13	32.73	0.87	0.4	0.03	20.99
HC(300, 600, 15)	63.37	4.47	2.15	30	0.85	0.36	0.029	22.45
HC(350, 600, 15)	68.23	4.32	2.03	25.41	0.76	0.28	0.026	24.7
HC(375, 600, 15)	66.15	2.68	1.92	29.25	0.49	0.33	0.025	20.96
HC(300, 600, 0)	61.75	4.26	2.09	31.91	0.83	0.39	0.029	21.26
HC(300, 600, 30)	62.73	4.38	2.14	30.75	0.84	0.37	0.029	21.97
HC(300, 600, 60)	64.5	4.33	2.12	29.05	0.81	0.34	0.028	22.8
Peat [94]	54.5	5.1	1.65	33.09	1.12	0.46	0.026	21.23
Lignite [94]	62.5	4.38	0.94	17.2	0.84	0.21	0.013	24.45

Where; HC(300, 300, 15) : set temperature of 300°C initial pressure of 300 psi and retention time of 15 min.

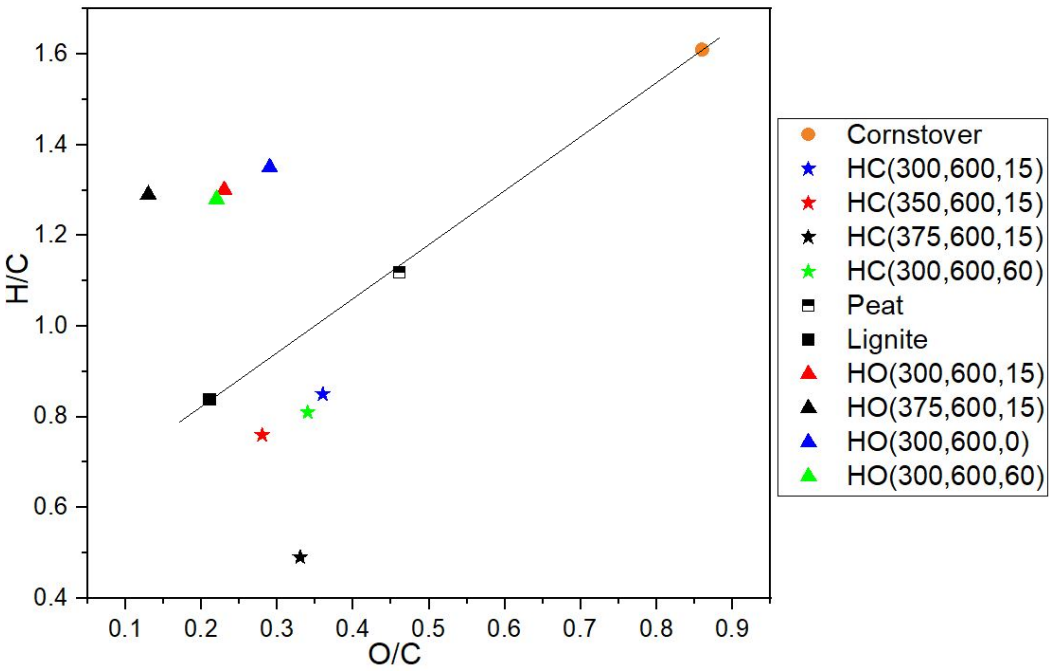

Figure 19 Van Krevelen diagram for corn stover, hydrochar and heavy oil

The elemental composition, HHV value, H/C, O/C and N/C ratio for HC obtained from HTL is depicted in Table 7. The HC obtained had higher carbon percent and HHV than raw feed ranging between 60.72 to 68.23 wt.% and 20.99 to 24.7 MJ/kg, respectively. Furthermore, the oxygen content was reduced in all HC than raw feed. The H/C and O/C ratio ranged between 0.49 - 0.87 and 0.28 - 0.39, which was significantly lower than corn stover. The N wt.% and N/C ratio was found to be higher for HC than raw feed. It can be observed that C wt.% and HHV value firstly increased on increasing temperature from 250 – 350 °C and decreased afterwards. With the increase in retention time, the C wt.% and HHV value increased. The HC obtained from these conditions had similar or even better properties such as C wt.% and HHV results than market available low-grade coal (peat and lignite). All hydrochar have an atomic ratio H/C to O/C lower than peat, as shown in Figure 19.

4.3.1.2 Oil

Table 8 Elemental composition and HHV value for HO and AO

Sample	C	H	N	O	H/C	O/C	N/C	HHV (MJ/kg)
Heavy Oil								
HO(300, 300, 15)	68.33	7.42	1.51	22.74	1.3	0.25	0.019	29.63
HO(250, 600, 15)	64.87	7.19	1.47	26.47	1.33	0.31	0.019	27.47
HO(300, 600, 15)	69.35	7.51	1.59	21.54	1.3	0.23	0.02	30.32
HO(375, 600, 15)	76.32	8.23	1.89	13.56	1.29	0.13	0.021	35.13
HO(300, 600, 0)	65.7	7.4	1.39	25.5	1.35	0.29	0.018	28.22
HO(300, 600, 60)	70.23	7.59	1.73	20.55	1.3	0.22	0.021	30.77
Aqueous Oil								
AO(300, 300, 15)	36.91	5.81	1.81	55.46	1.89	1.13	0.042	10.87
AO(250, 600, 15)	35.74	6.27	1.49	56.5	2.11	1.19	0.036	10.95
AO(300, 600, 15)	34.13	6.23	1.81	57.83	2.19	1.27	0.045	10.11
AO(375, 600, 15)	28.07	5.73	1.8	64.41	2.45	1.72	0.055	6.17
AO(300, 600, 0)	36.17	6.08	1.59	56.16	2.02	1.16	0.038	10.88
AO(300, 600, 60)	35.35	5.79	1.96	56.89	1.97	1.21	0.048	10.06

Where (300, 300, 15): set temperature of 300 °C initial pressure of 300 psi and retention time of 15 min.

Table 8 shows the elemental analysis and HHV results for different fraction of oil obtained from HTL at different experimental conditions for comparison. The characterization was carried out only for specific conditions of temperature, pressure and retention time. The HO obtained contained significantly high carbon content than raw feed. The H/C and O/C ratio was reduced in all HO than raw feed. For HO average H/C ratio was 1.31 and O/C ratio was 0.24. The experimental condition (375 °C, 600 psi, 15 min) had highest C wt.% and HHV value equivalent to 76.32 wt.% and 35.13 MJ/kg; additionally, it had lowest H/C and O/C ratio 1.29 and 0.13, respectively. Hence, it can be called as qualitatively optimum condition. For the condition (300 °C, 600 psi, 0 min) which was quantitatively optimum result the C wt.% and HHV value was 65.7 wt.% and 28.22 MJ/kg, respectively. Figure 19 shows with increase in temperature or retention time both H/C and O/C atomic ratio was decreased. Based on data presented in Figure 19, it can be concluded that with increase in temperature and retention time dehydration became more

intense. The total N wt.% in HO was higher than the raw feed for all conditions and sulphur was below detection limit. The results were supported by cited articles [27, 32].

The elemental analysis result shows that AO contain less carbon and more oxygen than raw feed. Furthermore, the HHV value of AO was found to be lower than feed and hence these fractions of products don't show promising results to carry out further analysis. Wu et al. [26] obtained similar result for aqueous phase oil denoted as LO1 in his study.

4.3.2 GC-TCD and GC-MS

The gaseous products obtained from reaction were analyzed using GC-TCD (Agilent 7890A). The gaseous products detected were a mixture of CO_2, CH_4, C_2H_6, C_2H_4, C_3H_6, C_4H_8, C_4H_6, C_5H_{12}, C_6H_{14}, C_6H_{12} and N_2.

Table 9 Summarized GC-MS analysis results for heavy oil fraction at different experimental conditions

Group of compounds	Area %					
	HO(250, 600, 15)	HO(300, 600, 0)	HO(300, 600, 15)	HO(300, 600, 60)	HO(350, 600, 15)	HO(375, 600, 15)
Ketones	9.57	7.13	2.09	3.33	2.54	6.69
Linear saturated HC	0.87	0.45	1.74	1.3	0.58	1.81
Linear unsaturated HC	-	0.71	7.6	7.47	5.52	9.91
Phenyl compounds	3.7	2.82	3.78	2.72	5.23	7.01
Phenol derivatives	77.62	56.42	77.47	73.82	81.49	70.56
Aldehyde	-	5.09	-	-	2.23	0.53
Fatty acids	-	8.67	-	-	-	-
Fatty acid alkyl esters	4.94	6.16	-	-	-	-
Others	3.7	12.55	7.32	11.37	2.4	3.49
Total area	100	100	100	100	100	100

In order to better understand the molecular composition of HO, it was analyzed on GC-MS. The summary of GC-MS analysis results of HO obtained at temperature 250, 300, 350, 375 °C and retention time 0, 15 and 60 min are tabulated in Table 9. The dark brown colored HO is a very complex mixture which builds many challenges in analysis and identification of compounds. The NIST 11 library used for identification provided detailed list of all possible similar structures lying in same retention time range and best set of compounds were selected based on literature review. The detailed list of possible compounds based on relative peak area is provided in the Appendix A Table A1.

For all mentioned conditions, HO had a relatively high percentage of phenol derivatives. The main phenol derivatives in HO obtained at temperature 250 to 350 °C were 2-Methoxy-phenol, 4-Ethyl-phenol, 4-Ethyl-2-methoxy-phenol and 2,6-Dimethoxy phenol. At 375 °C the major phenol derivatives observed were Phenol, 2-Methyl-phenol, 3-Methyl-phenol, 2,4-Dimethyl-phenol, 4-Ethyl-phenol and 2-Ethyl-6-methyl-phenol. It can be said that at 375 °C removal of oxygen has taken place as a fraction of oxy compounds is reduced which is supported by the reduced O wt.% obtained in CHNS analysis result and lower O/C atomic ratio presented in Figure 4. For longer retention time of 60 min and for higher temperature of 350 and 375 °C, long linear unsaturated chain of 1-Nonadecene and (Z)-9-Tricoscene were also detected. For HO (300,600,0) around 15 % relative area of peaks represented fatty acids and fatty acid alkyl esters derivatives, which were absent at higher temperature and longer retention time. Similar observation can also be made based on result presented in Gao et al. [88] for GC-MS of HO obtained from HTL of cellulose.

4.3.3 FTIR studies

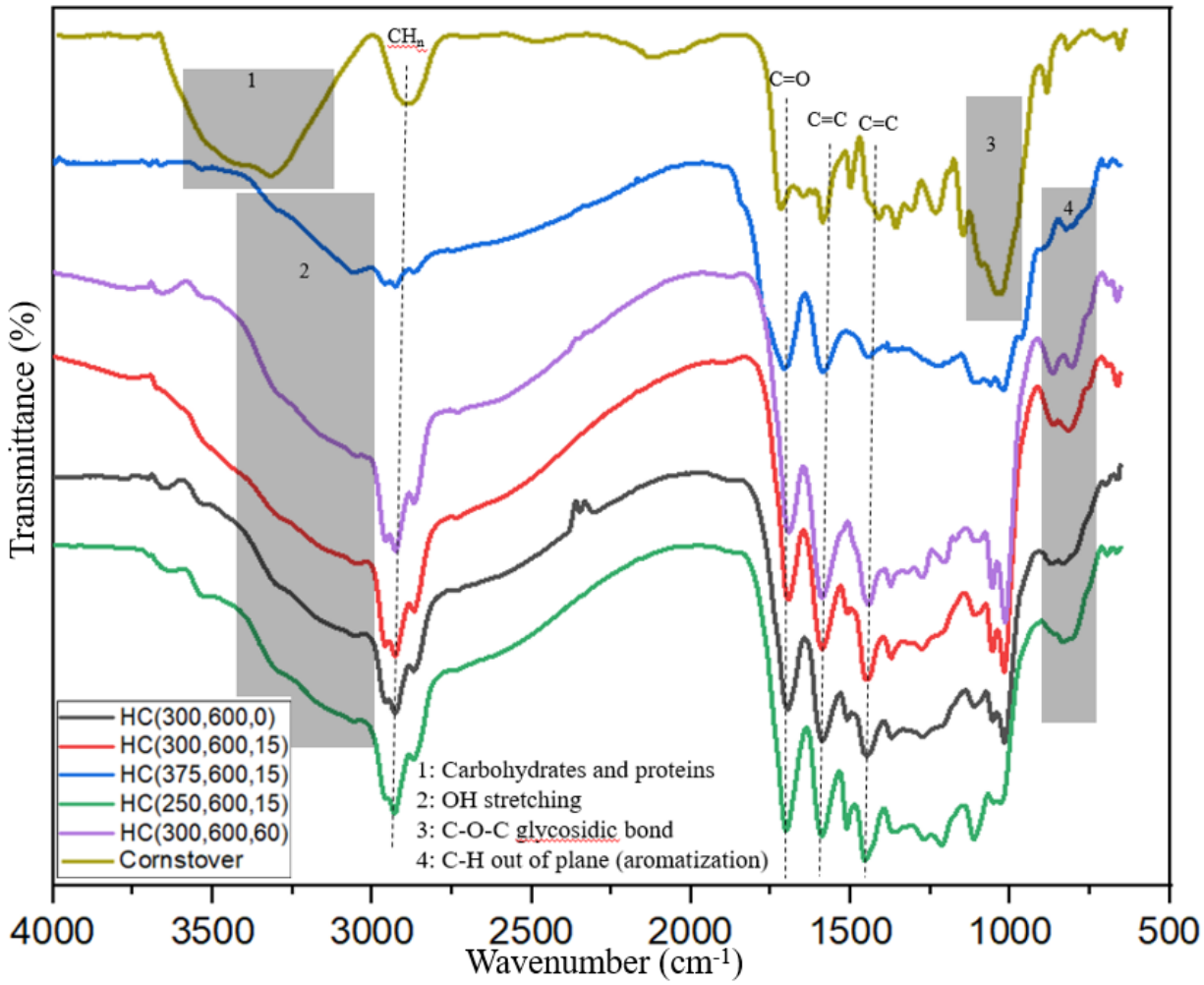

Figure 20 FTIR analysis results for raw corn stover and hydrochar from HTL.

The results of FTIR data for raw corn stover and hydrochar at different conditions of temperature, pressure and retention time are depicted in Figure 20. The FTIR results help us to understand the presence of different function groups and how the different process condition is affecting their presence in the hydrochar. The presence of broad absorbance in the range of 3500 to 3300 cm^{-1} in case of corn stover represents the presence of carbohydrates and proteins [23, 33], whereas, it dampens and completely disappears in hydrochar. Furthermore, the area under stretch in the range of 3500 – 3300 cm^{-1} decreases. The absorption band developed in hydrochar between

2900 – 3400 cm^{-1} corresponds to O–H stretching developed due to the presence of carboxylic or alcohol group. The peak 2850 – 3000 cm^{-1} corresponds to aliphatic C–H group; it is widely visible in raw feed and hydrochar. The intensity of peak increased in case of most of the hydrochar indicating breaking of cellulosic compounds into simpler aliphatic forms whereas for temperature 375 °C the peak decreases indicating shift of aliphatic bonds from simpler to complex aromatic bonds. The band between 1700 – 1750 cm^{-1} attributes to C=O stretching. The C=O vibration indicates the presence of carboxylic, ester, quinone, conjugated aldehyde, conjugated ketone, αβ unsaturated ester and aliphatic ketone groups. Zhu et al. [40] confirmed that lignin remains intact in some fraction by indicating the aromatic skeletal vibration and aryl-O stretching. Similar pattern of aromatic vibration near 1600 cm^{-1} and 1500 cm^{-1} along with the peaks near 1200 cm^{-1} attributing aryl-O stretching was observed in all the hydrochar confirming the presence of lignin. The existence of C=C was confirmed by the peak at 1450 cm^{-1} usually attributed to aromatic compounds. The stretch near 1150 – 1100 cm^{-1} corresponds to C–O stretching generally present in aliphatic ether and alcohol as well as represents C–O–C glycosidic bond present in cellulose; it can be found widely in corn stover and in some part for HC(250 °C) while it squeezes at higher temperature. The existence of some new absorbance peaks in HC near 750 – 850 cm^{-1} attributes to out of plane C–H bending giving support to formation of aromatic ring structure [39, 62].

4.3.4 Morphology of HC

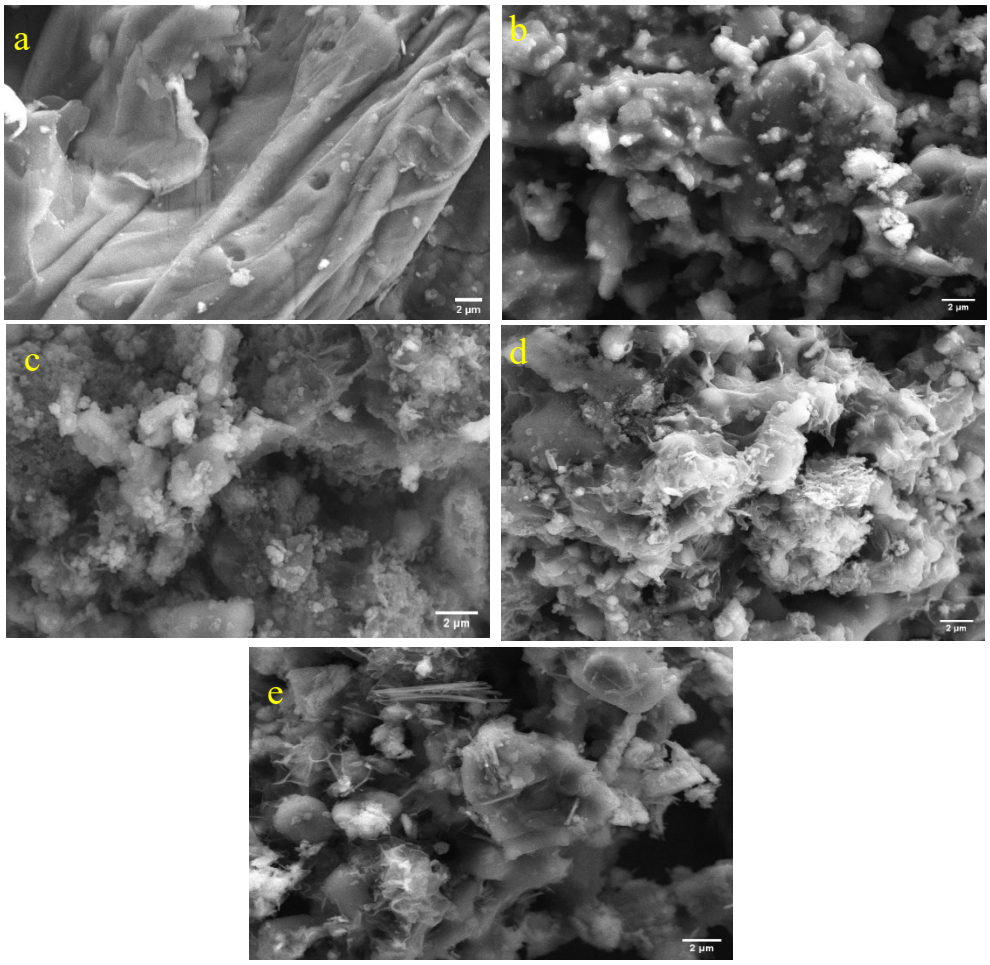

Figure 21 SEM of (a) corn stover, (b)HC(250, 600, 15) (c) HC(300, 600, 0), (d)HC(300, 600, 60), (e) HC(375, 600, 15)

The SEM images of corn stover and HC are shown in Figure 21. All the HC obtained from reactions showed thermal cracks whereas for corn stover a lumpy dense matrix was observed. At 250 ºC, HC showed evenly distributed microspheres of around 450 nm with very few cracks and bigger chunk of particles dominated on surface indicating start of cell disruption of hemicellulose and cellulose structure. On increasing temperature to 300 °C, the number of microspheres increased with a size range around 250 nm evenly distributed on surface; furthermore, surface

became more porous with increased thermal cracks. The presence of microsphere signifies oxygen containing functional groups [39, 63]. On further increasing temperature to 375 °C or increasing retention time to 60 min, multiple rod and filament shaped structure were observed with increased agglomerates. The increase in agglomerates at higher temperature could be because of the repolymerization reaction.

Table 10 BET surface area, average pore diameter and pore volume for hydrochar at different reaction condition

Sample	BET Surface area (m^2/g)	Average pore diameter (nm)	Pore volume (cm^3/g)
HC(250, 300, 15)	1.05	21.96	0.012
HC(300, 300, 15)	3.36	19.47	0.033
HC(350, 300, 15)	2.98	12.42	0.019
HC(375, 300, 15)	3.69	10.89	0.02
HC(250, 600, 15)	5.74	17.41	0.05
HC(300, 600, 15)	3.92	21.24	0.045
HC(350, 600, 15)	3.17	14.4	0.023
HC(375, 600, 15)	3.69	13	0.024

The BET surface area of HC was very less, ranging between 1.05-5.74 m^2/g; similar results were also observed by Fuertes et al. [97].

Chapter 5 : Conclusion and Future Work

5.1 Conclusion

A parametric study on HTL of corn stover showed that it to be a promising technique to produce biofuels. Distribution of different products was significantly affected by operating conditions. Highest conversion and yield of HO was 82.62 wt.% and 29.25 wt.%, respectively obtained at 300 °C, final pressure 2200 psi and 0 min. HO yield decreased with increase in temperature above 300 °C and retention time above 0 min. When performing HTL mainly for hydrochar, yield of HC was maximum at 350 °C. The increase in pressure negatively affect HC yield whereas retention time has little effect on it. The total gas formation increased at higher pressure, longer retention time, above 350 °C.

A series of analysis for bio-oil, hydrochar and gas were conducted using analytical techniques to understand the quality of products obtained at different conditions. The HO (375, 600, 15) had highest C of 76.32 wt.%, O/C value of 0.13 and HHV value of 35.13 MJ/kg. The HO is mainly composed of phenol derivatives, with some percentage of ketones, linear saturated and unsaturated hydrocarbons, and phenyl groups. At temperature, 250 and 300 °C fatty acids and fatty acid alkyl ester derivatives were also observed.

The HC (350, 600, 15) had highest C of 68.21 wt.%, O/C of 0.28 and HHV value of 24.7 MJ/kg, which is comparatively better than peat and lignite. The FTIR results showed, disappearing peaks of protein, carbohydrates and glycosidic bonds in hydrochar with increasing temperature; the O–H stretching indicated carboxylic and alcoholic groups and C=O absorption bend represented ester, aldehyde and ketone group. The C–H bending (750-850 cm^{-1}) indicated formation of aromatic rings in hydrochar. Based on the morphology, the HC has thermal cracks

and porous surface; presence of microsphere indicates formation of oxygen containing groups. The agglomerate formation at higher temperature was concluded to be due to repolymerization reactions.

5.2 Future work

- In the next step different solvents/additives can be tested along with water to understand their effect on the quality and yield of product.
- Study can be conducted on understanding the stability of bio-oil on prolonged exposure to atmospheric condition.
- More research is needed and recommended for upgrading the quality of bio-oil.

Bibliography

[1] M. R. Lotfalipour, M. A. Falahi, and M. Ashena, "Economic growth, CO2 emissions, and fossil fuels consumption in Iran," *Energy*, 2010.

[2] D. Pudasainee, V. Kurian, and R. Gupta, *CHAPTER 5. Application Status of Post-combustion CO2 Capture*, no. 2. The Royal Society of Chemistry, 2018.

[3] Boden, T.A., G. Marland and RJA. Global Fossil-Fuel CO2 Emissions. Carbon Dioxide Inf Anal Center, Oak Ridge Natl Lab US Dep Energy, Oak Ridge, Tenn, USA 2017. https://doi.org/10.3334/CDIAC/00001_V2017 .

[4] E. Stephens *et al.*, "Future prospects of microalgal biofuel production systems," *Trends Plant Sci.*, vol. 15, no. 10, pp. 554–564, 2010.

[5] United Nations, *[World population prospects 2019]*., no. 141. 2019.

[6] Energy Information Administration, "International Energy Outlook," *Outlook*, vol. 0484, no. July, pp. 70–99, 2019.

[7] W. De Jong and J. R. Van Ommen, "Biomass as a Sustainable Energy Source for the Future: Fundamentals of Conversion Processes," *Biomass as a Sustain. Energy Source Futur. Fundam. Convers. Process.*, vol. 9781118304, pp. 1–582, 2014.

[8] P. Basu, *Introduction-Biomass Gasification, Pyrolysis and Torrefaction*. Elsevier Inc., 2013.

[9] V. Khatri, F. Meddeb-Mouelhi, K. Adjallé, S. Barnabé, and M. Beauregard, "Determination of optimal biomass pretreatment strategies for biofuel production: Investigation of relationships between surface-exposed polysaccharides and their enzymatic conversion using carbohydrate-binding modules," *Biotechnol. Biofuels*, vol. 11, no. 1, pp. 1–16, 2018.

[10] E. Gatt, V. Khatri, J. Bley, S. Barnabé, V. Vandenbossche, and M. Beauregard, "Enzymatic hydrolysis of corn crop residues with high solid loadings: New insights into the impact of bioextrusion on biomass deconstruction using carbohydrate-binding modules," *Bioresour. Technol.*, vol. 282, no. March, pp. 398–406, 2019.

[11] R. A. Lee and J.-M. Lavoie, "From first- to third-generation biofuels: Challenges of producing a commodity from a biomass of increasing complexity," *Anim. Front.*, vol. 3, no. 2, pp. 6–11, 2013.

[12] M. Patel and A. Kumar, "Production of renewable diesel through the hydroprocessing of lignocellulosic biomass-derived bio-oil: A review," *Renew. Sustain. Energy Rev.*, vol. 58, pp. 1293–1307, 2016.

[13] A. Tursi, "A review on biomass: Importance, chemistry, classification, and conversion," *Biofuel Res. J.*, vol. 6, no. 2, pp. 962–979, 2019.

[14] J. S. Tumuluru, S. Sokhansanj, C. T. Wright, R. D. Boardman, and N. A. Yancey, "A review on biomass classification and composition, co-firing issues and pretreatment methods," *Am.*

Soc. Agric. Biol. Eng. Annu. Int. Meet. 2011, ASABE 2011, vol. 3, no. August 2011, pp. 2053–2083, 2011.

[15] E. Monedero, J. J. Hernández, and R. Collado, "Combustion-related properties of poplar, willow and black locust to be used as fuels in power plants," *Energies*, vol. 10, no. 7, pp. 1–11, 2017.

[16] Q. Zhai, F. Li, F. Wang, J. Xu, J. Jiang, and Z. Cai, "Liquefaction of poplar biomass for value-added platform chemicals," *Cellulose*, vol. 25, no. 8, pp. 4663–4675, 2018.

[17] C. Li *et al.*, "Hydrothermal liquefaction of desert shrub salix psammophila to high value-added chemicals and hydrochar with recycled processing water," *BioResources*, vol. 8, no. 2, pp. 2981–2997, 2013.

[18] Y. Yue, J. R. Kastner, and S. Mani, "Two-Stage Hydrothermal Liquefaction of Sweet Sorghum Biomass - Part 1: Production of Sugar Mixtures," *Energy and Fuels*, vol. 32, no. 7, pp. 7611–7619, 2018.

[19] A. Gollakota and P. E. Savage, "Hydrothermal Liquefaction of Model Food Waste Biomolecules and Ternary Mixtures under Isothermal and Fast Conditions," *ACS Sustain. Chem. Eng.*, vol. 6, no. 7, pp. 9018–9027, 2018.

[20] U. Schuchardt and F. de Assis Pereira Matos, "Liquefaction of sugar cane bagasse with formate and water," *Fuel*, vol. 61, no. 2, pp. 106–110, 1982.

[21] K. Ziemiński, I. Romanowska, M. Kowalska-Wentel, and M. Cyran, "Effects of hydrothermal pretreatment of sugar beet pulp for methane production," *Bioresour. Technol.*, vol. 166, pp. 187–193, 2014.

[22] T. Y. Ahmad, T. Hirajima, S. Kumagai, and K. Sasaki, "Production of solid biofuel from agricultural wastes of the palm oil industry by hydrothermal treatment," *Waste and Biomass Valorization*, vol. 1, no. 4, pp. 395–405, 2010.

[23] W. T. Chen *et al.*, "Co-liquefaction of swine manure and mixed-culture algal biomass from a wastewater treatment system to produce bio-crude oil," *Appl. Energy*, vol. 128, pp. 209–216, 2014.

[24] M. León, A. F. Marcilla, and Á. N. García, "Hydrothermal liquefaction (HTL) of animal by-products: Influence of operating conditions," *Waste Manag.*, vol. 99, pp. 49–59, 2019.

[25] T. H. Pedersen *et al.*, "Continuous hydrothermal co-liquefaction of aspen wood and glycerol with water phase recirculation," *Appl. Energy*, vol. 162, no. January, pp. 1034–1041, 2016.

[26] X. F. Wu, Q. Zhou, M. F. Li, S. X. Li, J. Bian, and F. Peng, "Conversion of poplar into bio-oil via subcritical hydrothermal liquefaction: Structure and antioxidant capacity," *Bioresour. Technol.*, vol. 270, no. September, pp. 216–222, 2018.

[27] S. Cheng, I. DCruz, M. Wang, M. Leitch, and C. Xu, "Highly efficient liquefaction of woody biomass in hot-compressed alcohol-water co-solvents," *Energy and Fuels*, vol. 24, no. 9, pp. 4659–4667, 2010.

[28] S. Karagöz, T. Bhaskar, A. Muto, Y. Sakata, T. Oshiki, and T. Kishimoto, "Low-

temperature catalytic hydrothermal treatment of wood biomass: Analysis of liquid products," *Chem. Eng. J.*, vol. 108, no. 1–2, pp. 127–137, 2005.

[29] S. Karagöz, T. Bhaskar, A. Muto, Y. Sakata, and M. A. Uddin, "Low-temperature hydrothermal treatment of biomass: Effect of reaction parameters on products and boiling point distributions," *Energy and Fuels*, vol. 18, no. 1, pp. 234–241, 2004.

[30] S. Li and X. Yang, *Biofuel production from food wastes*. 2016.

[31] X. Li, E. Mupondwa, S. Panigrahi, L. Tabil, S. Sokhansanj, and M. Stumborg, "A review of agricultural crop residue supply in Canada for cellulosic ethanol production," *Renew. Sustain. Energy Rev.*, vol. 16, no. 5, pp. 2954–2965, 2012.

[32] S. V. Vassilev, D. Baxter, L. K. Andersen, C. G. Vassileva, and T. J. Morgan, "An overview of the organic and inorganic phase composition of biomass," *Fuel*, vol. 94, pp. 1–33, 2012.

[33] M. Kumar, A. Olajire Oyedun, and A. Kumar, "A review on the current status of various hydrothermal technologies on biomass feedstock," *Renew. Sustain. Energy Rev.*, vol. 81, no. March 2017, pp. 1742–1770, 2018.

[34] F. Cherubini, "The biorefinery concept: Using biomass instead of oil for producing energy and chemicals," *Energy Convers. Manag.*, vol. 51, no. 7, pp. 1412–1421, 2010.

[35] S. Konsomboon, J. M. Commandre, and S. Fukuda, "Torrefaction of Various Biomass Feedstocks and Its Impact on the Reduction of Tar Produced during Pyrolysis," *Energy and Fuels*, vol. 33, no. 4, pp. 3257–3266, 2019.

[36] D. K. Shen, S. Gu, K. H. Luo, A. V. Bridgwater, and M. X. Fang, "Kinetic study on thermal decomposition of woods in oxidative environment," *Fuel*, vol. 88, no. 6, pp. 1024–1030, 2009.

[37] G. W. Huber, S. Iborra, and A. Corma, "Synthesis of transportation fuels from biomass: Chemistry, catalysts, and engineering," *Chem. Rev.*, vol. 106, no. 9, pp. 4044–4098, 2006.

[38] A. Demirbas, "Calculation of higher heating values of fatty acids," *Energy Sources, Part A Recover. Util. Environ. Eff.*, vol. 38, no. 18, pp. 2693–2697, 2016.

[39] H. Li *et al.*, "Liquefaction of rice straw in sub- and supercritical 1,4-dioxane-water mixture," *Fuel Process. Technol.*, vol. 90, no. 5, pp. 657–663, 2009.

[40] Z. Zhu, L. Rosendahl, S. S. Toor, D. Yu, and G. Chen, "Hydrothermal liquefaction of barley straw to bio-crude oil: Effects of reaction temperature and aqueous phase recirculation," *Appl. Energy*, vol. 137, pp. 183–192, 2015.

[41] T. Qu, W. Guo, L. Shen, J. Xiao, and K. Zhao, "Experimental study of biomass pyrolysis based on three major components: Hemicellulose, cellulose, and lignin," *Ind. Eng. Chem. Res.*, vol. 50, no. 18, pp. 10424–10433, 2011.

[42] C. Wall, C. Division, and C. Growth, "Cell Wall, Cell Division, and Cell Growth."

[43] L. Cao *et al.*, "Hydrothermal liquefaction of agricultural and forestry wastes: state-of-the-art review and future prospects," *Bioresour. Technol.*, vol. 245, no. August, pp. 1184–1193, 2017.

[44] R. M. ROWELL, R. PETERSSEN, and J. S. HAN, *Cell Wall Chemistry*. 2005.

[45] B. J. C. Duchemin, "Mercerisation of cellulose in aqueous NaOH at low concentrations," *Green Chem.*, vol. 17, no. 7, pp. 3941–3947, 2015.

[46] T. Minowa, F. Zhen, and T. Ogi, "Cellulose decomposition in hot-compressed water with alkali or nickel catalyst," *J. Supercrit. Fluids*, vol. 13, no. 1–3, pp. 253–259, 1998.

[47] E. Kamio, S. Takahashi, H. Noda, C. Fukuhara, and T. Okamura, "Effect of heating rate on liquefaction of cellulose by hot compressed water," *Chem. Eng. J.*, vol. 137, no. 2, pp. 328–338, 2008.

[48] C. Greenhalf, "Thermochemical characterisation of various biomass feedstock and bio-oil generated by fast pyrolysis," 2014.

[49] H. Chen, *Biotechnology of Lignocellulose*. 2014.

[50] J. K. Weng and C. Chapple, "The origin and evolution of lignin biosynthesis," *New Phytol.*, vol. 187, no. 2, pp. 273–285, 2010.

[51] W. Boerjan, J. Ralph, and M. Baucher, " L Ignin B Iosynthesis ," *Annu. Rev. Plant Biol.*, vol. 54, no. 1, pp. 519–546, 2003.

[52] C. M. Welker, V. K. Balasubramanian, C. Petti, K. M. Rai, S. De Bolt, and V. Mendu, "Engineering plant biomass lignin content and composition for biofuels and bioproducts," *Energies*, vol. 8, no. 8, pp. 7654–7676, 2015.

[53] D. W. F. Brilman, N. Drabik, and M. Wądrzyk, "Hydrothermal co-liquefaction of microalgae, wood, and sugar beet pulp," *Biomass Convers. Biorefinery*, vol. 7, no. 4, pp. 445–454, 2017.

[54] M. K. Akalin, K. Tekin, and S. Karagöz, "Hydrothermal liquefaction of cornelian cherry stones for bio-oil production," *Bioresour. Technol.*, vol. 110, pp. 682–687, 2012.

[55] S. Anouti, G. Haarlemmer, M. Déniel, and A. Roubaud, "Analysis of Physicochemical Properties of Bio-Oil from Hydrothermal Liquefaction of Blackcurrant Pomace," *Energy and Fuels*, vol. 30, no. 1, pp. 398–406, 2016.

[56] M. Déniel, G. Haarlemmer, A. Roubaud, E. Weiss-Hortala, and J. Fages, "Optimisation of bio-oil production by hydrothermal liquefaction of agro-industrial residues: Blackcurrant pomace (Ribes nigrum L.) as an example," *Biomass and Bioenergy*, vol. 95, pp. 273–285, 2016.

[57] Z. Liu, A. Quek, S. Kent Hoekman, and R. Balasubramanian, "Production of solid biochar fuel from waste biomass by hydrothermal carbonization," *Fuel*, vol. 103, pp. 943–949, 2013.

[58] F. Wang *et al.*, "Hydrothermal liquefaction of Litsea cubeba seed to produce bio-oils," *Bioresour. Technol.*, vol. 149, pp. 509–515, 2013.

[59] L. Yang, L. Nazari, Z. Yuan, K. Corscadden, C. C. Xu, and Q. S. He, "Hydrothermal liquefaction of spent coffee grounds in water medium for bio-oil production," *Biomass and Bioenergy*, vol. 86, pp. 191–198, 2016.

[60] C. Wang, J. Pan, J. Li, and Z. Yang, “Comparative studies of products produced from four different biomass samples via deoxy-liquefaction,” *Bioresour. Technol.*, vol. 99, no. 8, pp. 2778–2786, 2008.

[61] S. Yin, R. Dolan, M. Harris, and Z. Tan, “Subcritical hydrothermal liquefaction of cattle manure to bio-oil: Effects of conversion parameters on bio-oil yield and characterization of bio-oil,” *Bioresour. Technol.*, vol. 101, no. 10, pp. 3657–3664, 2010.

[62] L. Garcia Alba *et al.*, “Hydrothermal treatment (HTT) of microalgae: Evaluation of the process as conversion method in an algae biorefinery concept,” *Energy and Fuels*, vol. 26, no. 1, pp. 642–657, 2012.

[63] U. Jena, K. C. Das, and J. R. Kastner, “Effect of operating conditions of thermochemical liquefaction on biocrude production from Spirulina platensis,” *Bioresour. Technol.*, vol. 102, no. 10, pp. 6221–6229, 2011.

[64] V. Kumar *et al.*, “Low-temperature catalyst based Hydrothermal liquefaction of harmful Macroalgal blooms, and aqueous phase nutrient recycling by microalgae,” *Sci. Rep.*, vol. 9, no. 1, pp. 1–9, 2019.

[65] Z. Shuping, W. Yulong, Y. Mingde, I. Kaleem, L. Chun, and J. Tong, “Production and characterization of bio-oil from hydrothermal liquefaction of microalgae Dunaliella tertiolecta cake,” *Energy*, vol. 35, no. 12, pp. 5406–5411, 2010.

[66] B. Wang, Y. Huang, and J. Zhang, “Hydrothermal liquefaction of lignite, wheat straw and plastic waste in sub-critical water for oil: Product distribution,” *J. Anal. Appl. Pyrolysis*, vol. 110, no. 1, pp. 382–389, 2014.

[67] C. Xu and J. Lancaster, “Conversion of secondary pulp/paper sludge powder to liquid oil products for energy recovery by direct liquefaction in hot-compressed water,” *Water Res.*, vol. 42, no. 6–7, pp. 1571–1582, 2008.

[68] D. Y. C. Leung, X. Wu, and M. K. H. Leung, “A review on biodiesel production using catalyzed transesterification,” *Appl. Energy*, vol. 87, no. 4, pp. 1083–1095, 2010.

[69] D. Kim, “Physico-chemical conversion of lignocellulose: Inhibitor effects and detoxification strategies: A mini review,” *Molecules*, vol. 23, no. 2, 2018.

[70] R. C. Saxena, D. K. Adhikari, and H. B. Goyal, “Biomass-based energy fuel through biochemical routes: A review,” *Renew. Sustain. Energy Rev.*, vol. 13, no. 1, pp. 167–178, 2009.

[71] P. McKendry, “Energy production from biomass (part 2): conversion technologies,” *Fuel*, vol. 83, pp. 47–54, 2002.

[72] T. Nussbaumer, “Combustion and Co-combustion of Biomass: Fundamentals, Technologies, and Primary Measures for Emission Reduction,” *Energy and Fuels*, vol. 17, no. 6, pp. 1510–1521, 2003.

[73] M. Balat, M. Balat, E. Kirtay, and H. Balat, “Main routes for the thermo-conversion of biomass into fuels and chemicals. Part 1: Pyrolysis systems,” *Energy Convers. Manag.*, vol. 50, no. 12, pp. 3147–3157, 2009.

[74] J. Singh and S. Gu, “Biomass conversion to energy in India-A critique,” *Renew. Sustain. Energy Rev.*, vol. 14, no. 5, pp. 1367–1378, 2010.

[75] T. Ogi, S.-Y. Yokoyama, and K. Koguchi, “Direct liquefaction of wood by catalyst (part 1), effects of pressure, temperature, holding time and wood/catalyst/water ratio on oil yield,” *Sekiyu Gakkaishi (Journal Japan Pet. Institute)*, vol. 28, no. 3, pp. 239–245, 1984.

[76] J. Akhtar, S. K. Kuang, and N. A. S. Amin, “Liquefaction of empty palm fruit bunch (EPFB) in alkaline hot compressed water,” *Renew. Energy*, vol. 35, no. 6, pp. 1220–1227, 2010.

[77] T. Minowa, F. Zhen, and T. Ogi, “Cellulose decomposition in hot-compressed water with alkali or nickel catalyst,” *J. Supercrit. Fluids*, vol. 13, no. 1–3, pp. 253–259, 1998.

[78] A. Hammerschmidt *et al.*, “Catalytic conversion of waste biomass by hydrothermal treatment,” *Fuel*, vol. 90, no. 2, pp. 555–562, 2011.

[79] K. Tekin, M. K. Akalin, and S. Karagöz, “The effects of water tolerant Lewis acids on the hydrothermal liquefaction of lignocellulosic biomass,” *J. Energy Inst.*, vol. 89, no. 4, pp. 627–635, 2016.

[80] L. Zhang, P. Champagne, and C. (Charles) Xu, “Bio-crude production from secondary pulp/paper-mill sludge and waste newspaper via co-liquefaction in hot-compressed water,” *Energy*, vol. 36, no. 4, pp. 2142–2150, 2011.

[81] Y. Ishikawa and S. Saka, “Chemical conversion of cellulose as treated in supercritical methanol,” *Cellulose*, vol. 8, no. 3, pp. 189–195, 2001.

[82] C. S. Theegala and J. S. Midgett, “Hydrothermal liquefaction of separated dairy manure for production of bio-oils with simultaneous waste treatment,” *Bioresour. Technol.*, vol. 107, pp. 456–463, 2012.

[83] J. Akhtar and N. A. S. Amin, “A review on process conditions for optimum bio-oil yield in hydrothermal liquefaction of biomass,” *Renew. Sustain. Energy Rev.*, vol. 15, no. 3, pp. 1615–1624, 2011.

[84] Z. Liu, A. Quek, S. Kent Hoekman, and R. Balasubramanian, “Production of solid biochar fuel from waste biomass by hydrothermal carbonization,” *Fuel*, vol. 103, pp. 943–949, 2013.

[85] J. Gan, W. Yuan, N. O. Nelson, and S. C. Agudelo, “Hydrothermal conversion of corn cobs and crude glycerol,” *Biol. Eng.*, vol. 2, no. 4, pp. 197–210, 2010.

[86] A. Kruse and A. Gawlik, “Biomass conversion in water at 330-410 °C and 30-50 MPa. Identification of key compounds for indicating different chemical reaction pathways,” *Ind. Eng. Chem. Res.*, vol. 42, no. 2, pp. 267–279, 2003.

[87] F. Goudriaan *et al.*, “Thermal Efficiency of the HTU® Process for Biomass Liquefaction,” *Prog. Thermochem. Biomass Convers.*, pp. 1312–1325, 2008.

[88] Y. Gao, X. H. Wang, H. P. Yang, and H. P. Chen, “Characterization of products from hydrothermal treatments of cellulose,” *Energy*, vol. 42, no. 1, pp. 457–465, 2012.

[89] Y. Wang *et al.*, “Effects of solvents and catalysts in liquefaction of pinewood sawdust for

the production of bio-oils," *Biomass and Bioenergy*, vol. 59, pp. 158–167, 2013.

[90] K. Tekin, S. Karagöz, and S. Bektaş, "Hydrothermal liquefaction of beech wood using a natural calcium borate mineral," *J. Supercrit. Fluids*, vol. 72, pp. 134–139, 2012.

[91] S. Karagöz, T. Bhaskar, A. Muto, Y. Sakata, T. Oshiki, and T. Kishimoto, "Low-temperature catalytic hydrothermal treatment of wood biomass: Analysis of liquid products," *Chem. Eng. J.*, vol. 108, no. 1–2, pp. 127–137, 2005.

[92] C. Xu and T. Etcheverry, "Hydro-liquefaction of woody biomass in sub- and super-critical ethanol with iron-based catalysts," *Fuel*, vol. 87, no. 3, pp. 335–345, 2008.

[93] M. Vaezi and A. Kumar, "Development of correlations for the flow of agricultural residues as slurries in pipes for Bio-refining," *Biosyst. Eng.*, vol. 127, pp. 144–158, 2014.

[94] P. Basu, "Biomass Gasification, Pyrolysis and Torrefaction: Practical Design and Theory. 3.6.2 Proximate Analysis," 2013.

[95] M. Liang, K. Zhang, P. Lei, B. Wang, C. M. Shu, and B. Li, "Fuel properties and combustion kinetics of hydrochar derived from co-hydrothermal carbonization of tobacco residues and graphene oxide," *Biomass Convers. Biorefinery*, 2019.

[96] M. Sevilla and A. B. Fuertes, "The production of carbon materials by hydrothermal carbonization of cellulose," *Carbon N. Y.*, vol. 47, no. 9, pp. 2281–2289, 2009.

[97] A. B. Fuertes *et al.*, "Chemical and structural properties of carbonaceous products obtained by pyrolysis and hydrothermal carbonisation of corn stover," *Aust. J. Soil Res.*, vol. 48, no. 6–7, pp. 618–626, 2010.

Appendix A

Table A1

GC-MS results for HO obtained at different reaction conditions

RT	Name	Area %					
		HO (250,600,15)	HO (300,600,0)	HO (300,600,15)	HO (300,600,60)	HO (350,600,15)	HO (375,600,15)
8.51	2-Methyl-2-cyclopenten-1-one	0.45	-	0.89	-	2.54	0.3
11.89	1,3-Dimethyl-1-cyclohexene	-	-	-	0.67	-	-
11.95	Phenol	-	5.66	1.18	2.6	4.87	5.95
13.18	2,3-Dimethyl-2-cyclopenten-1-one	-	-	1.2	3.33	-	5.23
13.98	2,3,4-Trimethyl-2-cyclopenten-1-one	-	-	-	-	-	1.16
14.26	2-Methyl-phenol	-	-	-	0.89	1.79	5.21
14.87	2-Methyl-3-methylene-cyclopentanecarboxaldehyde	-	-	-	3.01	2.23	-
14.89	2,4-Dimethyl-2,3-pentadiene	-	-	-	-	-	2.11
14.91	2-Methyl-2,3-hexadiene	-	0.36	2.29	-	-	-
14.96	2-Methoxy-phenol	9.79	5.41	8.15	7.13	6.01	-
15.04	3-Methyl-phenol	-	-	-	-	-	8.96
15.33	1-Isopropylcyclohex-1-ene	-	-	0.38	1.71	0.58	1.27
15.47	3-Phenyl-2-propyn-1-ol	-	-	-	-	-	0.82
15.79	2,6-Dimethyl-phenol	-	-	-	-	-	0.65
16.21	3,4-Heptadiene	-	-	-	-	-	1.68
16.6	(E)-1-Phenyl-1-butene	-	-	-	-	-	0.25
16.68	2-Methylbicyclo [3.2.1] octane	-	-	-	-	-	0.63
16.85	2-Ethyl-phenol	-	-	-	-	-	2.79
17.15	2,4-Dimethyl-phenol	-	-	-	-	0.54	2.51
17.76	4-Ethyl-phenol	26.68	0.57	32.39	35.14	40.41	24.32
18.03	4-Methyl-benzenemethanol	-	-	0.38	-	-	3.25

18.16	Creosol	-	1.73	2.25	3.79	2.46	-
18.24	4-Hydroxy-benzeneethanol	0.28	-	-	-	-	-
18.48	4-Phenyl-, (E)-3-buten-2-one	-	-	-	-	-	0.42
18.62	1,6-Dimethylhepta-1,3,5-triene	-	-	-	-	-	0.56
18.9	2,3-Dimethylhydroquinone	-	-	-	-	-	0.45
19.45	2,4,6-Trimethyl-phenol	-	-	-	-	-	0.71
19.68	2-Ethyl-6-methyl-phenol	-	-	-	-	3.4	4.33
20.09	3-Methylenecycloheptene	-	-	1.56	1.77	-	-
20.1	(E) - 3-Dodecen-1-yne	-	-	-	-	0.94	-
20.37	2-Propyl-phenol	-	-	-	-	-	4.83
20.51	4-Ethyl-2-methoxy-phenol	22.73	4.31	25.43	21.92	17.98	4.24
21.37	Benzocycloheptatriene	-	-	-	-	-	1.21
21.39	5-Methylisophthalonitrile	-	-	-	0.91	-	-
21.4	2-Methyl-naphthalene	-	-	1.04	-	1.58	-
21.65	2,5-Diethylphenol	-	-	-	-	2.2	2.03
21.69	4-Acetylanisole	-	-	-	0.5	-	-
21.81	2-Methyl-6-propylphenol	-	-	-	-	-	0.5
22.58	2,3-Dihydro-1H-inden-5-ol	-	-	-	-	-	1.05
22.59	2,6-Dimethoxy-phenol	17.25	31.38	6.73	-	-	-
22.64	3-Amino-2,6-dimethoxypyridine	-	-	-	4.26	-	-
22.89	2-Methoxy-4-propyl-phenol	-	-	1.34	1.84	1.83	0.25
22.9	2',4'-Dihydroxypropiophenone	-	1.08	-	-	-	-
23.27	Cyclotetradecane	0.87	-	1.74	1.3	-	0.62
23.29	Cyclododecane	-	0.45	-	-	-	-
23.68	2-propenyl-benzene	-	-	-	-	-	1.06
23.77	1,5,6,7-Tetramethylbicyclo [3.2.0] hepta-2,6-diene	-	-	-	-	-	1.48
24.1	Vanillin	-	0.53	-	-	-	-
24.49	2-Allyl-4-methylphenol	-	-	-	-	-	0.52
24.67	5-Methylthiophene-2,3-dicarbonitrile	-	-	-	-	-	0.6
24.78	5-Formyl-2,4-dimethyl-pyrrole-3-carbonitrile	-	-	-	-	-	0.55
25.01	3-Hydroxy-4-methoxybenzoic acid	-	6.31	-	-	-	-
25.03	1,5-Heptadiyne	-	-	2.45	-	-	-

25.06	2-Butynedioic acid, di-2-propenyl ester	1.28	-	-	-	-	-
25.27	6-Methyl-4-indanol	-	-	-	-	-	1.25
25.91	Pentadecane	-	-	-	-	-	0.56
26.19	1-(3-Hydroxy-4-methoxyphenyl)-ethanone	0.41	-	-	-	-	-
26.2	6-Methyl-5-(1-methylethyl)-5-hepten-3-yn-2-ol	-	0.34	-	-	-	-
26.24	2,8-Dimethyl-indolizine	-	-	-	-	-	1.3
26.61	trans-4-Methoxycinnamaldehyde	-	-	-	-	-	0.53
26.62	Dihydrofuranno(3,2-f) coumaran	-	1.62	-	-	-	-
26.85	5-Tert-butylpyrogallol	-	6.03	-	-	-	-
26.86	1,2,3-Trimethoxy-5-methyl-benzene	3.7	-	2.36	-	-	-
26.86	4-Ethylbiphenyl	-	-	-	2.72	-	-
26.87	1-Methyl-4-(phenylmethyl)-benzene	-	-	-	-	0.71	-
27.14	2,3-Dihydro-2,2-dimethyl-3,7-benzofurandiol	-	0.79	-	-	-	-
27.41	Chloroacetic acid, 2-naphthyl ester	-	-	-	-	1.23	-
27.74	1-Methyl-3,4-dihydroisoquinoline	-	-	-	-	-	1.05
28.07	Z-8-Hexadecene	-	-	0.92	1.27	-	-
28.08	5-Amino-6-piperidinofurazano[3,4-b] pyrazine	-	0.34	-	-	-	-
28.64	2-Hydroxy-4-isopropyl-7-methoxytropone	-	1.03	-	-	-	-
28.74	2-Mercaptobenzothiazole	-	-	2.82	3.19	-	-
28.76	3,4-dimethoxy-mandelic acid methyl ester	-	4.62	-	-	-	-
28.76	1-(2,5-Dimethoxyphenyl)-propanol	-	-	-	-	2.94	-
28.76	(2E,4Z)-3-methyl-4-propyl-2,4-hexadienedioic acid dimethyl ester	3.66	-	-	-	-	-
30.1	1-Methyl-3-(2-phenylethenyl)-, (E)-benzene	-	1.2	-	-	-	-
30.17	4-Hydroxy-3,5-dimethoxy-benzaldehyde	-	5.09	-	-	-	-
30.17	3-methoxy-2-naphthalenol	0.88	-	-	-	-	-
30.92	3-(4-Hydroxy-3-methoxyphenyl)- (E)-2-propenoic acid	-	1.54	-	-	-	-
31.02	7-Methyl-6-tridecene	-	-	-	-	1.46	1.27
31.75	1-(4-hydroxy-3,5-dimethoxyphenyl)-ethanone	8.71	1.73	-	-	-	-
32.55	1-(2,4,6-Trihydroxyphenyl)2-pentanone	-	2.97	-	-	-	-
33.81	3,5,7-Trihydroxy-2H-1-benzopyran-2-one	-	0.32	-	-	-	-
34.99	5-Amino-6,8-dimethoxyquinoline	-	2.51	-	-	-	-

38.53	n-Hexadecanoic acid	-	2.36	-	-	-	-
38.68	8-Amino-6,7-dimethoxy-4-methylquinoline	-	1.47	-	-	-	-
42.55	5-(1-Naphthyl)-4-phenyl-2-thiazolamine	1.77	-	-	-	-	-
45.86	(Z)-9-Tricosene	-	-	-	-	-	1.54
45.86	1-Nonadecene	-	-	-	2.06	3.12	-